

**ONSET AND CHARACTERISATION OF CHAOS  
IN A TWO DIMENSIONAL NONLINEAR  
DETERMINISTIC MODEL**

**K. P. HARIKRISHNAN**

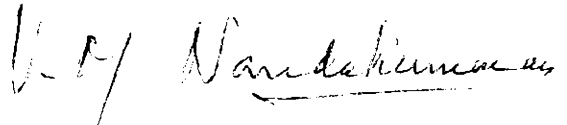
THESIS SUBMITTED IN  
PARTIAL FULFILMENT OF THE REQUIREMENTS  
FOR THE DEGREE OF  
**DOCTOR OF PHILOSOPHY**

DEPARTMENT OF PHYSICS  
COCHIN UNIVERSITY OF SCIENCE AND TECHNOLOGY  
COCHIN - 682 022

1989

C E R T I F I C A T E

Certified that the work reported in the present thesis is based on the bonafide work done by Mr. K.P. Harikrishnan under my guidance in the Department of Physics, Cochin University of Science and Technology and has not been included in any other thesis submitted previously for the award of any degree.



Cochin-22,  
3-11-'89

V.M. Nandakumaran  
(Supervising Teacher)

D E C L A R A T I O N

Certified that the work presented in this thesis is based on the original work done by me under the guidance of Dr. V.M. Nandakumaran, Reader, Department of Physics, Cochin University of Science and Technology and has not been included in any other thesis submitted previously for the award of any degree.

Cochin-22  
3-11-'89

  
K.P. Harikrishnan

TO MY FATHER AND MOTHER

## A C K N O W L E D G E M E N T S

First of all, I wish to express my sincere gratitude to my guide Dr. V.M. Nandakumaran, Reader, Department of Physics, Cochin University of Science and Technology for his help and encouragement. He has been a constant source of inspiration throughout.

I am also thankful to Prof. K. Babu Joseph, Head of the Department of Physics, Cochin University of Science and Technology and Prof. M.G. Krishna Pillai, former Head of the Department of Physics for their help and co-operation.

Thanks are also due to

- Dr. G. Ambika and Dr. A.T. Reghunath for some useful discussions.
- Prof. R. Pratap, Prof. K.L. Sebastian and Dr. V.P.N. Nampoori for their interest in my work.
- all my colleagues of the Department who have helped me at some stage or other during the course of my research. I have shared many a pleasant moment with Mr. J. Sreekumar, Mr. M.P. Joy, Mr. Jose Mathew, Prof. K.V. Thomas, Mr. Johny Isaac, Mr. V.J. Peter, Mr. M. Ravindranathan, Mr. K.N. Madhusoodanan and Mr. Titus K.M.
- Ms. Rajalakshmi for a neat typing of this thesis.
- the CSIR, New Delhi for financial assistance.

# C O N T E N T S

	Page No.
Preface	i - vi
I DETERMINISTIC CHAOS: AN INTRODUCTION	
1.1 What is chaotic dynamics?	2
1.2 Simple methods to identify chaos	6
1.3 Important routes for the transition to chaos	13
1.4 The quantitative measures	18
1.5 Importance of deterministic chaos	30
II MATHEMATICAL MODELS OF CHAOTIC DYNAMICS	
2.1 One dimensional mappings : The logistic map	33
2.2 Higher dimensional models	36
2.3 One dimensional maps and universality	42
2.4 A 'modulated' logistic map	52
III BIFURCATIONS AND UNIVERSALITY IN THE MODULATED LOGISTIC MAP	
3.1 Bifurcation structure and linear stability analysis	56
3.2 Approximate renormalisation methods and calculation of universal constants	68
3.3 Universal ordering of periodic windows	75
IV OBSERVATION AND CHARACTERISATION OF CHAOS	
4.1 Lyapunov exponents of the map	85
4.2 The strange attractors of the map	93
4.3 Fractal and information dimensions	97
V CONCLUDING REMARKS	106
References	111

## P R E F A C E

This is a report of the investigations carried out by the author under the guidance of Dr. V.M. Nandakumaran in the Department of Physics, Cochin University of Science and Technology, during the period 1985-89. It essentially deals with the onset and characterisation of chaos in a nonlinear deterministic model.

The discovery that the evolution of low dimensional nonlinear systems with a set of completely deterministic equations can be very complex or 'chaotic' has triggered an upsurge of research interest among physicists today. The study of simple nonlinear models describing various natural phenomena has resulted in the emergence of a new area of research now known as 'deterministic chaos'. Within a short period of time, a number of important breakthroughs have been achieved including the establishment of universal properties at the transition to chaos and the development of the important concept of a 'strange attractor'. For

the time being most of our knowledge of chaotic behaviour comes from studies on discrete nonlinear mappings. An important example is the so called logistic equation given by

$$X_{t+1} = 4 \lambda X_t (1 - X_t)$$

which maps the unit interval on the real line into itself and  $\lambda \in [0,1]$  is a control parameter determining the asymptotic behaviour of the system.

Now, eventhough one dimensional maps have been thoroughly investigated, studies on higher dimensional noninvertible maps are comparatively very few and their properties are less well understood today.

We introduce a logistic type model in two dimensions

$$\begin{aligned} X_{t+1} &= 4 \lambda_t X_t (1 - X_t) \\ \lambda_{t+1} &= 4 \mu \lambda_t (1 - \lambda_t) \end{aligned}$$

where the role of the control parameter is played by  $\mu \in [0,1]$ . In other words, we consider a situation where the parameter of the logistic map at any instant depends on its value at the previous instant in a nonlinear way. As suggested by Ruelle, many time evolutions occurring in nature are of this type with 'adiabatically fluctuating parameters'. The



work reported in the thesis is devoted to the study of this 'modulated' logistic map. We investigate this model thoroughly from the view point of deterministic chaos and establish many interesting properties using analytical as well as numerical methods.

The thesis contains five chapters. First chapter provides a brief introduction to the subject of deterministic chaos. In this, we discuss the basic ideas of deterministic chaos and their importance in the study of nonlinear dynamical systems. A brief discussion of the period doubling and other commonly observed routes to chaos has been included. Moreover, the concepts of Lyapunov Exponent and fractal dimension, which are important quantitative measures of chaos are also introduced.

In Chapter II, certain simple models which have played a central role in the development of the subject are presented. We then give a brief review of the universal properties of one dimensional maps. Then the modulated logistic map is introduced which forms the subject matter for subsequent chapters. The importance of this model in understanding the chaotic behaviour of certain higher dimensional systems of current interest is also indicated.

In Chapter III, we study the onset of chaos in the modulated logistic map. It is shown that, as the parameter  $\mu$  is increased, the map turns chaotic following an infinite cascade of period doubling bifurcations. By plotting the bifurcation structure of the map in the  $(X_t, \mu)$  plane, we show that it is modified qualitatively as well as quantitatively from the first bifurcation onwards. A linear stability analysis is performed to determine the fixed points of the map analytically. A very interesting property of our map is the existence of the universal behaviour of Feigenbaum at the transition to chaos. By using the approximate renormalisation methods due to Derrida et al and Helleman, we calculate the bifurcation ratio  $\delta$  and the scaling factor  $\alpha$  of the map. Their values suggest that the map should be included in the universality class of Feigenbaum. A detailed analysis of the 3-dimensional bifurcation structure of the map in the region  $\mu > \mu_\infty$  gives numerical evidence for the fact that the map has infinite number of periodic windows which are arranged along the parameter axis exactly as in the case of the logistic map. The importance of this result lies in the fact that this ordering - known as Sarkovskii ordering - is thought to be characteristi

of only one hump maps and so far no higher dimensional maps are known to show this property.

In Chapter IV, we study the chaotic region of the map making use of some important quantitative measures. We mainly concentrate on the Lyapunov exponent and the fractal dimension which are quite general and are applicable to a wide spectrum of problems. The former is the rate of exponential divergence of nearby trajectories and hence is a measure of the loss of predictability, where as the latter is a quantitative measure of the strangeness of the attractor. We calculate the two Lyapunov exponents of the map for a number of parameter values and show that the Lyapunov exponent along the X-direction is always negative. It is then shown that the map can generate uncountable number of strange attractors in the unit square. We present numerical plot of the attractors for various values of  $\mu$  and the self similar structure is explicitly shown in one case. The fractal dimension  $D_0$  and the information dimension  $D_1$  of a number of strange attractors corresponding to various values of  $\mu$  have been calculated and in most of the cases, found to lie between 1 and 2 confirming the fractal structure.

The last Chapter provides summary and evaluation of investigations presented in the preceding chapters. An important conclusion that we derive is that the 'modulated' logistic map can be considered as an analogue of the logistic map in two dimensions. Other important results are also specified and possibilities for future investigations are indicated.

Part of the investigations presented in the thesis has provided materials for the following publications.

1. Universal behaviour in a 'modulated' logistic map, Phys. Lett. A 125 (1987) 465.
2. Bifurcation structure and Lyapunov exponents of a 'modulated' logistic map, Pramana - J. Phys. 29 (1987) 533.
3. Evidence for the existence of Sarkovskii ordering in a two dimensional map, Phys. Lett. A 133 (1988) 305.
4. Universal properties in a 'modulated' logistic map, Proceedings of the International Conference on Mathematical Modelling in Science and Technology - Eds. N.V.C. Swamy, P. Achuthan and S.N. Majhi (Tata McGraw-Hill, New Delhi, 1988) p. 243-250.
5. An analogue of the logistic map in two dimensions, Phys. Lett. A (in press).

## I DETERMINISTIC CHAOS : AN INTRODUCTION

Nature is full of phenomena which we call 'chaotic', the weather being a prime example. What we mean by this is that we cannot predict it to any significant accuracy, either because the system is inherently complex, or because some of the governing factors are not deterministic. However, during recent years it has become clear that random behaviour can occur even in very simple systems with very few number of degrees of freedom, without any need for complexity or indeterminacy. The discovery that chaos can be generated even with the help of systems having completely deterministic rules - often models of natural phenomena - has stimulated a lot of research interest recently. Not that this chaos has no underlying order, but it is of a subtle kind, that has taken a great deal of ingenuity to unravel. In the present thesis, we introduce a new nonlinear model, a 'modulated' logistic map, and analyse it from the view point of 'deterministic chaos'. This chapter provides a brief introduction to the subject of deterministic chaos and its importance in the study of nonlinear dynamical systems.

### 1.1 What is chaotic dynamics?

There are various kinds of processes occurring in nature, such as, physical, chemical, biological, ecological etc. with each of them representing phenomenon different from the other ones. We hope to model these processes by dynamical systems, where the state of the system is represented by a point, say  $X$ , on some 'manifold' and evolves in time  $t$  according to a certain rule given by a set of equations. A dynamical system can, in general, be written either as a set of coupled first order ordinary differential equations [1] of the form

$$\frac{d\vec{X}}{dt} = \vec{V}(\vec{X}) \quad (1)$$

or as a set of coupled difference equations or 'maps' of the form

$$X_{t+1} = F(X_t) \quad (2)$$

If  $\vec{X}$  and  $\vec{V}$  have  $N$  components, then the phase space of the system (1) is  $N$ -dimensional and the trajectory of  $\vec{X}$  is called an  $N$ -dimensional flow. The fact that all equations are assumed to be of first order is not a restriction as it might seem at first sight: a differential system can always be brought into this form by introducing additional

variables. The system (1) is autonomous, which means that right hand side is explicitly independent of time. Again this is not really a restriction : a nonautonomous system can be transformed into an autonomous system by the introduction of additional variables. In the case of equations (2), the system is observed at equal intervals of time instead of following the trajectory continuously. This is essentially what we do in many contexts where, only the qualitative behaviour of the solutions of the system is of interest. A very simple example is the study of the evolution of the population in a closed area encountered in population biology [2]. These equations can also be obtained as a Poincaré section [1] of a flow in phase space.

Dynamical systems can be broadly classified into two, conservative or Hamiltonian systems and dissipative systems and the two do not lead to the same class of problems. For a conservative system, the phase space volume remains invariant during the time evolution of the system. Certain questions of practical importance, like the evolution of the solar system, especially its long term stability for example, come under this heading. This subject requires specific mathematical techniques [1,6] notably because of the determining

influence on the initial conditions. Dissipative systems, on the other hand, are systems with an internal friction which entails a continuous decrease of energy during the evolution. As a result, the phase space volume gets contracted and hence the asymptotic ( $\text{time} \rightarrow \infty$ ) motion of a dissipative system takes place on a subspace of the total phase space, called an 'attractor'. In other words, there exists an asymptotic limit of the solutions, a limit on which an initial condition has no direct influence. We will be mostly interested in dissipative systems here.

Given a dynamical system, one is primarily interested in the solution for a very long time compared to the time scale of the system, that is, the asymptotic behaviour of the solutions. When we say that a system is 'chaotic', we mean that its long time behaviour cannot be predicted with sufficient accuracy. Chaos arises due to an intrinsic property of a dynamical system and, nonlinearity is a necessary but not sufficient condition for the system to be chaotic.

At this stage, it is necessary to distinguish between the so called 'random' and 'chaotic' motions



in the context of dynamical systems. The former is used for problems in which we truly do not know the input forces or we only know some statistical measures of the parameters whereas the latter is reserved for the unpredictable evolution of deterministic physical and mathematical systems for which there are no random inputs or parameters. In other words, 'deterministic chaos' can most conveniently be thought of as a dynamical phenomenon, the situation being such that even an infinitesimal error regarding the state of a completely deterministic system at one time still renders impossible the task of predicting the future history of the system. It is the discovery that relatively simple nonlinear systems such as, for example, the logistic map [2] or the Lorenz system [3] can lead to highly complex behaviour that has stimulated a great deal of interest in the study of chaotic dynamical systems.

The question now naturally arises as to what is the factor responsible for chaos in a completely deterministic system? The answer lies on a fundamental property of certain nonlinear systems. It is observed that for certain Parameter regimes they show a 'sensitive dependence on initial conditions', a property by which the distance between two initially

close trajectories in phase space diverge 'exponentially' in time. If the initial condition of a deterministic system is accurately specified, one can in principle determine precisely the future evolution of the system. However, for a system possessing the above property, an infinitesimal error in the initial condition will get amplified exponentially in time resulting in a totally different evolution of the system. It is then evident that prediction becomes impossible for such a system since the initial conditions cannot, in practice, be specified with infinite accuracy.

## 1.2 Simple methods to identify chaos

When, as a result of an experiment or numerical simulation, we have a time dependent signal  $X(t)$  - called a time series - one of the essential tasks is to determine the kind of evolution that produced it. Are we dealing with a perfectly well defined periodic motion? Or is it more or less a linear superposition of several different periods or even something entirely different?

To answer these questions, we must use objective methods of analysis which help to identify and characterise a dynamical regime. Here we discuss some of the important methods which are commonly used to identify chaos.

One simple method is the calculation of the correlation function [5]. For a chaotic system, the correlation function decays exponentially in time since the correlation between two close points in phase space decays exponentially.

#### The power spectrum and FFT

Another widely used tool to distinguish regular and chaotic motion is the 'power spectrum' [4] which we now discuss in some detail. The power spectrum, say  $S(\omega)$ , of a signal  $X(t)$  is defined as the square of its Fourier amplitude per unit time. Typically, it measures the amount of energy per unit time (ie, the power) contained in the signal as a function of the frequency  $\omega$ . One can also define  $S(\omega)$  as the Fourier transform of the time correlation function  $\langle X(0) X(t) \rangle$  equal to the average over  $\tau$  of  $X(\tau) X(t+\tau)$ . The appearance of the power spectrum clearly indicates the way in which the signal evolves in time, that is, whether it is periodic, quasiperiodic or chaotic. For a

periodic system with frequency  $w$ , it will have a peak at  $w$  and also at its harmonics  $2w, 3w \dots$ . A quasiperiodic system with basic frequencies  $w_1, \dots w_k$  will have peaks at these positions and also at all linear combinations with integer coefficients. In the case of a chaotic system, we will have a continuous power spectrum. This is usually interpreted as corresponding to an infinite number of modes. However, there are in fact two possibilities: we are either in the presence of a system that 'explores' an infinite number of dimensions in phase space, or we have a system that evolves nonlinearly on a finite dimensional attractor [7]. Eventhough both alternatives are possible, the second appears frequently in practice.

Very often, the signal  $X(t)$  is measured by sampling and discretising, which provides a discrete sequence of real numbers regularly spaced at time intervals of  $\Delta t$ . This sequence of numbers is necessarily finite, containing  $N$  values for a total length of time  $t_{\max} = N \Delta t$  with the choice of  $N$  and  $\Delta t$  determined by practical considerations.

Now, the first step towards obtaining the power spectrum is the calculation of the discrete Fourier transform of these finite number of sampled points.

Suppose that we have  $N$  consecutive sampled values

$$h_k \equiv h(t_k), t_k = k \Delta t, k = 0, 1, 2 \dots N-1.$$

For simplicity, we assume that  $N$  is even. The discrete Fourier transform of these  $N$  points is given by

$$H_n = \sum_{k=0}^{N-1} h_k e^{2\pi i k n / N}$$

where the index  $n$  varies from  $-\frac{N}{2}$  to  $\frac{N}{2}$ . Once  $H_n$  is calculated, the power spectral density  $P_k$  can be obtained as  $|H_n|^2$ . The standard method to compute  $H_n$  is to define a complex number  $W$  as

$$W = e^{2\pi i / N}$$

which allows  $H_n$  to be written as

$$H_n = \sum_{k=0}^{N-1} W^{nk} h_k.$$

In other words, the vector of  $h_k$ 's is multiplied by a matrix whose  $(n,k)^{th}$  element is the constant  $W$  to the power  $nk$ . The matrix multiplication produces a vector result whose components are the  $H_n$ 's. This matrix multiplication evidently requires  $N^2$  complex multiplications. Thus in practice, the task of computing  $H_n$  becomes extremely difficult for large  $N$ . On the other hand, it is naturally advantageous to choose  $N$  large for a faithful representation of the signal.

Here, an algorithm called the 'fast Fourier transform (FFT)' comes to our help. Briefly, the method is as follows: The discrete Fourier transform of length  $N$  is rewritten as the sum of two discrete Fourier transforms, each of length  $N/2$ . One of the two is formed from the even numbered points of the original  $N$ , the other from the odd numbered points.

$$\begin{aligned}
 H_n &= \sum_{k=0}^{N-1} e^{2\pi i k n / N} h_k \\
 &= \sum_{k=0}^{N/2-1} e^{2\pi i k n / (N/2)} h_{2k} \\
 &\quad + W^n \sum_{k=0}^{N/2-1} e^{2\pi i k n / (N/2)} h_{2k+1} \\
 &= H_n^e + W^n H_n^o
 \end{aligned}$$

where  $H_n^e$  is the  $n^{\text{th}}$  component of the Fourier transform of length  $N/2$  formed from the even components of the original  $h_k$ 's and  $H_n^o$  is the corresponding transform formed from the odd components. The transforms  $H_n^e$  and  $H_n^o$  are periodic in  $n$  with length  $N/2$ . So each can be repeated through two cycles to obtain  $H_n$ .

The crucial point here is that the method can be used recursively. Having reduced the problem of computing  $H_n$  to that of computing  $H_n^e$  and  $H_n^o$ , the same reduction can be performed on  $H_n^e$  to the problem of computing the transform of its  $N/4$  even numbered input data and  $N/4$  odd numbered data. Now, the

easiest case will obviously be the one in which the original  $N$  is an integer power of 2. Then the process can be continued until we have subdivided the data to transform of length one. So the whole algorithm will be of order  $N \log_2 N$  instead of  $N^2$  which simplifies the task considerably. For a detailed discussion of FFT, see [8].

### The Poincare section

This is a very ingenious method employed frequently to study the qualitative features of the solutions of a dynamical system. The solutions to the system of differential equations (1) have an analytic expression only in particular well defined situations where the flow is integrable. If the flow is not integrable, as is usually the case, we must study each solution by following its trajectory in phase space. This task can be very much simplified by using a method developed by Henri Poincaré [1].

If we are interested only in the asymptotic behaviour of the solutions, then it is fruitful to observe only the points of intersection of the trajectory with a suitably chosen surface, say  $S$ , rather than directly studying the solutions in  $\mathbb{R}^n$ . The intersection is taken only when the trajectories cross  $S$  in the same direction. Starting with an initial

condition, we thus obtain a set of points, say  $P_0, P_1, P_2 \dots$ , comprising the "Poincaré section" - that is, a graph in  $(n-1)$  dimensions. The transformation leading from one point to the next is a continuous mapping  $T$  of  $S$  into itself called the "Poincaré map":

$$P_{k+1} = T(P_k) = T(T(P_{k-1})) = T^2(P_{k-1}) = \dots$$

Since the solution is unique, the point completely determines  $P_1$ , which in turn determines  $P_2$  and so on. Since the converse is also true, that is, since  $P_k$  also uniquely determines  $P_{k-1}$ , the mapping  $T$  is invertible. So, the Poincaré section replaces the continuous time evolution with a discrete time mapping where, the time interval between two successive points is, in general, not a constant.

The method of Poincaré sections has some obvious advantages over the study of continuous flows. First of all, we pass from a flow in  $R^n$  to a mapping in  $R^{n-1}$ , reducing the number of coordinates by one. Secondly, since time is discretised, the task of numerical integration of the system of differential equations are now reduced to the iteration of a set of algebraic equations.

Finally, by construction, the Poincaré section and map have the same kind of topological



properties as the flow from which they arise. For example, if the flow is dissipative, then  $T$  contracts areas in the plane  $S$  and if it is conservative,  $T$  also conserves areas. Moreover, if the flow has an attractor, its structural characteristics are also found in the Poincaré section. The appearance of the Poincaré section clearly shows the kind of asymptotic behaviour of the system. For example, if the solution is periodic with a definite period, the Poincaré section reduces to a single point which is the fixed point of the mapping  $T$ . If the trajectory is inscribed on a torus, the corresponding Poincaré section will lie on an organised curve, such as a circle in the case of a biperiodic regime. A more or less random or complicated distribution of points indicates the presence of a chaotic trajectory.

The simple methods that we have mentioned above only help to provide certain qualitative evidence for chaos and an extensive analysis of the chaotic state can be performed only with the help of specific quantitative measures discussed in sec. 1.4 below.

### 1.3 Important routes for the transition to chaos

As we have already seen, the asymptotic motion of a dissipative system takes place on a subspace of the total phase space, called an attractor,

on which the initial condition has no direct influence. Usually, a dissipative dynamical system will contain a set of control parameters which can be thought to represent the interaction of the system with the surroundings. The values of these parameters determine the asymptotic behaviour of the system and depending on their values, the behaviour may either be periodic or chaotic. The phenomenon by which the system changes from one stable state to another by the variation of a control parameter is called a 'bifurcation'. It is seen that a series of bifurcations take place before the system turns chaotic at a critical value of the parameter. An adequate understanding of the processes or routes by which a system turns chaotic is, of course, important for a systematic analysis of the chaotic state. In the case of low dimensional dissipative systems, a regular motion means motion on a simple attractor, such as, a fixed point, a limit cycle or a biperiodic orbit (torus). In fact, for one and two dimensional dissipative flows, the fixed point and limit cycle are the only possible attractors [6]. There are mainly three types of bifurcations [4,6] observed in such systems as shown in figure 1, where  $\mu$  represents

a single parameter. In fig. 1(a), a pair of stable and unstable (dashed line) attractors are created as the parameter crosses a critical value  $\mu_0$ , where as no stable attractors existed for  $\mu < \mu_0$ .

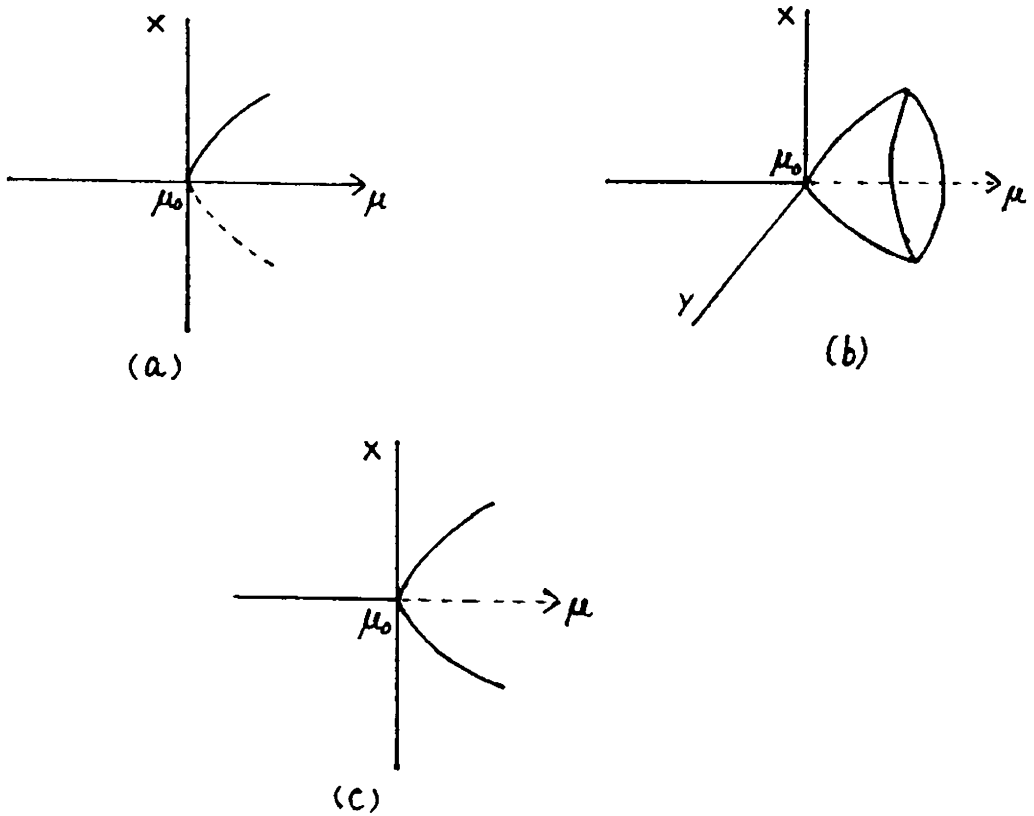


Fig. 1 Bifurcations in low dimensional dissipative flows

This type of bifurcation is called a 'tangent' bifurcation. Sometimes the topological nature of an existing attractor undergoes a change at the bifurcation point. For example, a fixed point

loses stability and a limit cycle is formed as shown in fig. 1(b). This is called a 'Hopf' bifurcation. In higher dimensional systems, a limit cycle may be replaced by a torus through the Hopf bifurcation. In the third type of bifurcation shown in fig. 1(c), a fixed point (a periodic cycle) becomes unstable and two new stable fixed points (a periodic cycle of twice the period) are formed. This is known as a 'pitch fork' bifurcation. Note that in the last case, only the periodicity of an existing attractor has doubled and no new stable state is actually created. Hence, it is also called a 'period doubling' bifurcation.

Depending on the type of bifurcations involved, there are three commonly observed routes by which a transition from regular to chaotic motion can occur in dissipative systems. These are the quasiperiodic route or Ruelle-Takens-Newhouse Scenario [9,10], the intermittency route or Pomeau-Manneville Scenario [11] and the period doubling route or Feigenbaum Scenario [12,13]. The basic mechanisms involved in each of these scenarios are illustrated below.

Route	Mechanism
Quasiperiodic	<p>Stationary point <math>\xrightarrow{\text{(Hopf)}}</math> Singly periodic orbit <math>\xrightarrow{\text{(Hopf)}}</math> Doubly periodic orbit</p> <p>Stationary point <math>\xrightarrow{\text{Chaos}}</math> Chaos</p>
Intermittency	<p>Stationary point <math>\xrightarrow{\text{(Hopf)}}</math> Singly periodic orbit <math>\xrightarrow{\text{(Inverse tangent bifurcation)}}</math> Chaos</p>
Period doubling	<p>Stationary point <math>\xrightarrow{\text{(Hopf)}}</math> Singly periodic orbit (Period T) <math>\xrightarrow{\text{(Pitchfork)}}</math> Singly periodic orbit (Period 2T) <math>\xrightarrow{\text{(Pitchfork)}}</math> Singly periodic orbit (Period 4T) <math>\xrightarrow{\text{(Pitchfork)}}</math> Chaos</p>

These routes have been analysed in detail using various mathematical techniques, such as renormalisation, and a number of quantitative measures characterising the transition to chaos have been obtained which are supported by experiments [4,14]. In fact, one reason for the current interest in the study of chaotic systems is the discovery of certain 'universal' properties in their transition to chaos. Such properties do not depend on the details of a particular model, but are true for a whole class of systems satisfying some general criteria. In the subsequent chapters, we will study the period doubling route in detail and the universal properties associated with it.

#### 1.4 The quantitative measures

So far we have discussed the basic properties of a chaotic system and the important routes by which simple deterministic systems can become chaotic. As the next important step in their analysis, we now discuss briefly how to describe and characterise a chaotic state. It has already been mentioned that the only possible attractors of one and two dimensional dissipative flows are the fixed points and the limit cycles. Consequently, their behaviour cannot be

chaotic. However, for 3-dimensional dissipative flows and the related 2-dimensional maps, it has been shown that attractors with very complicated geometric structures can exist. These structures are typically characterised by a fractional dimension [15] and are usually called 'strange attractors'[9]. The existence of a nontrivial attractor can be understood as follows.

We know that for a system to be chaotic, it should possess the property of 'sensitive dependance on initial conditions.' Also, for a dissipative system, the overall phase space volume is contracted by the time evolution. But this does not mean that the lengths are contracted in 'all' direction. Some direction may be stretched, provided some others are so much contracted that the final volume is smaller than the initial volume. This seemingly trivial remark has profound consequences. It implies that the final motion may be unstable 'within the attractor'. This instability usually manifests itself by an exponential separation of orbits (as time goes on) of points which are initially very close to each other on the attractor. The exponential separation takes place in the direction

of stretching, and an attractor having this stretching property is called a ''strange attractor''. It should be stressed that the 'strangeness' refers to the dynamics on the attractor and not to its geometry [7]. Since the attractor is in general bounded, exponential separation can only hold as long as distances are small. Evidence for the existence of a strange attractor was first given by Lorenz [3] using his now famous Lorenz model (see chapter II). This attractor is shown in fig.2. The complicated structure of the attractor is evident from the figure. The trajectory continues to wind around and around, without ever settling down to either periodic or stationary behaviour. It has now been established that chaos in dissipative systems is caused by the dynamics on a strange attractor.

### Fractal Dimension

The strange attractor is a complicated manifold in phase space. It is known to possess a ''self similar'' geometric structure. That is, the many-leaved structure of the attractor repeats itself on finer and finer scales. The most important property of a self similar structure is that its dimensionality could, in general, have noninteger values.



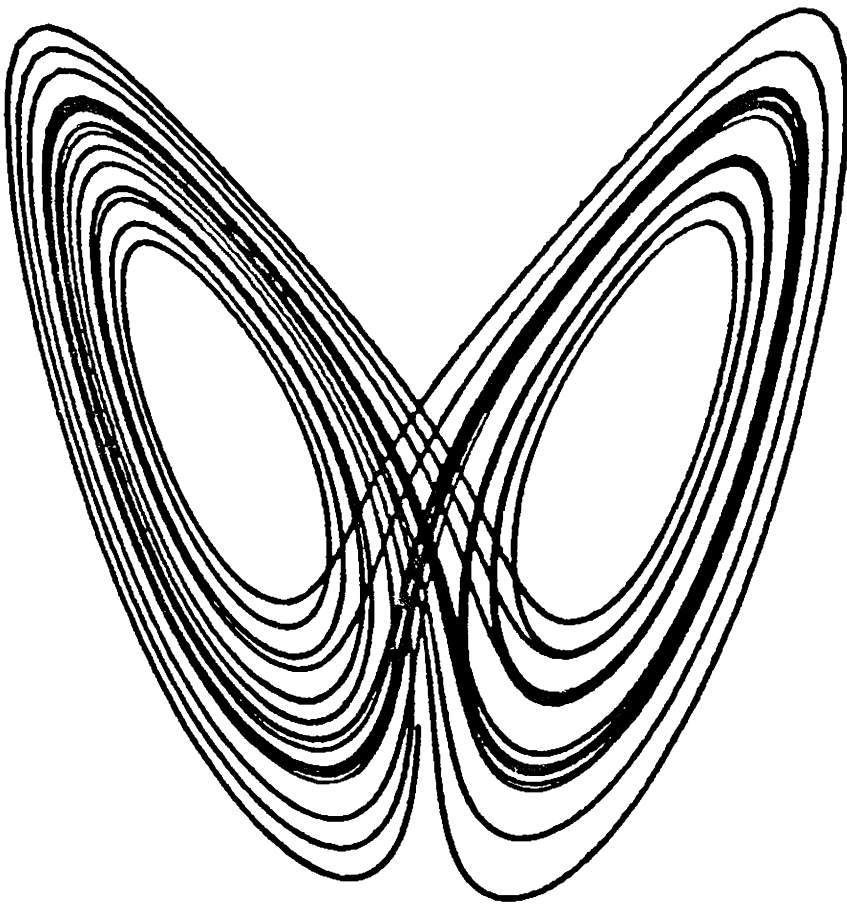


Fig. 2 The Lorenz attractor which is the first known example of a strange attractor

Let us now see how the definition of a dimension can be generalised to include the concept of a fractional dimension. We define the dimension of a subset  $S$  of an  $N$ -dimensional space as [6]:

$$D(S) = \lim_{\epsilon \rightarrow 0} \frac{\ln M(\epsilon)}{\ln (1/\epsilon)} \quad (3)$$

where  $M(\epsilon)$  is the minimum number of  $N$ -dimensional cubes of side  $\epsilon$  needed to cover the subset. For small  $\epsilon$ , this definition implies

$$M(\epsilon) \sim K \epsilon^{-D} . \quad (4)$$

The definition gives the dimensions of a point, a line and an area embedded in a 2-dimensional space their usual values of 0,1 and 2 respectively. This however does not rule out the possibility that the dimension of the set be a noninteger. As the simplest example, let us consider the Cantor set [15,6]. It is a compact metric space that is totally disconnected, uncountable and may have zero measure. It has a fractional dimension  $0 < D < 1$  and displays rescaling invariance; that is, a subset of the set, when properly magnified, looks like the original set. This structure has a close correspondence with that of a strange attractor and give considerable insight into

some of the general properties of the attractor. Consider a segment, say  $T_0$ , formed by the closed interval  $[0,1]$ . Delete the open (excluding the end points) interval  $(1/3, 2/3)$  called the "middle third", thus forming the set  $T_1$  consisting of two disconnected segments  $[0,1/3]$  and  $[2/3,1]$ . Delete the middle thirds of each of these two segments, thus forming  $T_2$  with four segments. Continue this process indefinitely constructing  $T_3, T_4, \dots$ . The Cantor set  $T$  is the intersection of all the  $T_n$ 's. Loosely speaking, the intersection is the "limiting  $T_n$ ".

From the construction, we see that  $T_n$  consists of  $M = 2^n$  disjoint intervals each of length  $\epsilon = 1/3^n$ . Applying eqn. (3), the dimension of  $T$  is

$$D = \lim_{n \rightarrow \infty} \frac{\ln 2^n}{\ln 3^n} = 0.630.$$

It is easy to see that  $T$  is uncountable and has measure zero:

$$\lim_{n \rightarrow \infty} \epsilon M = \left(\frac{2}{3}\right)^n \rightarrow 0.$$

There do exist in nature innumerable objects whose dimension is typically a noninteger. They are

called 'fractals' and are said to possess a 'fractal dimension'. It was Mandelbrot [15,16] who undertook a detailed mathematical study of these objects and coined the term 'fractal geometry' to denote their structure. The theory of fractals is now widely applied to understand the structure and dynamics of chaotic attractors. The fractal dimension is sometimes also referred to as Hausdorff dimension [15].

For a strange attractor, one can in fact, define an infinite number of generalised dimensions  $D_q$  [17]. Of these, the most important ones are  $D_0$  and  $D_1$  which represent two general types of dimensions.  $D_0$  depends only on the metric properties of the attractor and gives the usual fractal dimension whereas  $D_1$  depends on the frequency with which a typical trajectory visits different regions of the attractor and is called the 'dimension of the natural measure', more commonly known as the 'information dimension'. These are discussed in detail below with respect to our model. Extensive discussion on the generalised dimensions of strange attractors and their mathematical properties, such as, their relation to the Lyapunov exponents, are given in the reviews by Farmer et.al [18] and by Eckmann and Ruelle [7].

### Lyapunov Characteristic Exponent

Probably the most important quantitative measure of chaos is the Lyapunov characteristic exponent which plays a crucial role in the theory of both Hamiltonian and dissipative dynamical systems [6]. Roughly speaking, Lyapunov exponent (LE) is the mean exponential rate of divergence of nearby trajectories of a chaotic system in phase space and provides an easily computable quantitative measure of the degree of chaos. For stable periodic orbits, it measures the rate of convergence towards the stable attractor. The theory of LEs was first applied to characterise stochastic trajectories by Oseledec [19]. The connection between LEs and exponential divergence was given by Benettin et.al [20] who also developed the procedure for computing the LEs [21]. Following Lichtenberg and Lieberman [6], we now define the LEs for the flow  $\vec{X}(t)$  generated by an autonomous first order system,

$$\frac{d X_i}{dt} = V_i(\vec{X}), \quad i = 1, \dots M. \quad (5)$$

Consider a trajectory in the M-dimensional phase space and a nearby trajectory with initial conditions  $X_0$  and  $X_0 + \Delta X_0$  respectively, as shown in fig. 3.

These evolve with time yielding the tangent vector

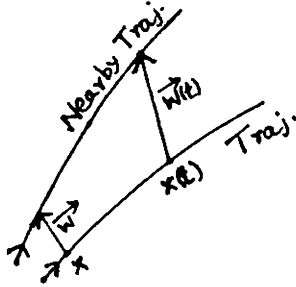


Fig. 3 Definition of Lyapunov exponents

$\vec{\Delta X}(X_0, t)$ , with its Euclidean norm

$$d(X_0, t) = ||\vec{\Delta X}(X_0, t)||.$$

Writing for convenience  $\vec{w} = \vec{\Delta X}$ , the time evolution for  $\vec{w}$  is found by linearising (5) to obtain

$$\frac{d\vec{w}}{dt} = \vec{M}(X(t)) \cdot \vec{w} \quad (6)$$

where  $\vec{M} = \frac{\partial \vec{V}}{\partial X}$  (7)

is the Jacobian matrix of  $\vec{V}$ . We now introduce the mean exponential rate of divergence of two initially close trajectories,

$$\sigma(X_0, w) = \lim_{t \rightarrow \infty} \lim_{d(0) \rightarrow 0} \left(\frac{1}{t}\right) \ln \frac{d(X_0, t)}{d(X_0, 0)}. \quad (8)$$

It can be shown that  $\sigma$  exists and is finite.

Furthermore, there is an M-dimensional basis  $\{\hat{e}_i\}$

of  $\vec{w}$  such that for any  $\vec{w}$ ,  $\sigma$  takes on one of the  $M$  (possibly nondistinct) values

$$\sigma_i(X_0) = \sigma(X_0, \hat{e}_i) \quad (9)$$

which are the Lyapunov characteristic exponents. It follows that for an  $M$ -dimensional system, there exist  $M$   $\sigma$ s which can be ordered by size,

$$\sigma_1 \geq \sigma_2 \geq \dots \geq \sigma_M.$$

The system is said to be chaotic if the largest LE  $\sigma_1 > 0$ .

The exponents  $\sigma_i$  are called Lyapunov exponents of order 1. The concept can be generalised to describe the mean rate of exponential growth of  $p$ -dimensional volume in the tangent space, where  $p \leq M$ . If  $V_p$  is the volume of a  $p$ -dimensional parallelepiped whose edges are the vectors  $\vec{w}_1, \vec{w}_2, \dots, \vec{w}_p$ , then

$$\sigma^{(p)}(X_0, V_p) = \lim_{t \rightarrow \infty} \left( \frac{1}{t} \right) \ln \frac{||V_p(X_0, t)||}{||V_p(X_0, 0)||} \quad (10)$$

defines a LE of order  $p$ . It can also be shown that  $\sigma^{(p)}$  is simply the sum of the  $p$  largest LEs of

order 1. For  $p = M$ , we obtain the mean exponential rate of growth of the phase space volume as

$$\overline{\sigma}^{(M)} = \sum_{i=1}^M \overline{\sigma}_i \quad (11)$$

For a conservative flow, we have  $\sum_i \overline{\sigma}_i = 0$ , while for a dissipative flow, this sum must be negative.

As in the case of flows, the LEs of maps also can be defined through equation (8), with  $t$  replaced by the number of iterations  $N$  and  $\vec{M}$  given by the Jacobian matrix of the map. If  $\wedge_i(N)$  are the eigen values of the product of the Jacobian matrices at the  $N$  iterates, then the LEs are given by

$$\overline{\sigma}_i = \lim_{N \rightarrow \infty} \frac{1}{N} \ln |\wedge_i(N)| \quad (12)$$

To see how an expression for the LE can be obtained explicitly, consider the ID map

$$X_{n+1} = f(X_n) \quad (13)$$

Consider two initial conditions separated by a distance  $\xi$ . After  $N$  iterations, we have



$\varepsilon \rightarrow e^{N\sigma(X_0)} \varepsilon$  , where  $\sigma(X_0)$  is the LE of the map. That is,

$$e^{N\sigma(X_0)} = \frac{|f^N(X_0) - f^N(X_0 + \varepsilon)|}{\varepsilon}$$

Assuming  $\varepsilon$  to be infinitesimal,

$$\begin{aligned} e^{N\sigma(X_0)} &= \lim_{\varepsilon \rightarrow 0} \frac{|f^N(X_0) - f^N(X_0 + \varepsilon)|}{\varepsilon} \\ &= \left| \frac{df^N(X_0)}{dX_0} \right| \end{aligned} \quad (14)$$

For  $N \rightarrow \infty$ , we have

$$\sigma(X_0) = \lim_{N \rightarrow \infty} \frac{1}{N} \ln \left| \frac{df^N(X_0)}{dX_0} \right| . \quad (15)$$

Using the chain rule of functional differentiation, one can easily show that

$$\sigma(X_0) = \lim_{N \rightarrow \infty} \frac{1}{N} \ln \left| \prod_{i=0}^{N-1} f'(X_i) \right| \quad (16)$$

Equation (12) is the generalised version of this expression for higher dimensional maps.

It can also be shown that the sum of the positive LEs is proportional to the average amount of information lost by the system in unit time. Only for reasonably simple dynamical systems, such as the 1D maps, can the LEs be estimated analytically. But

the numerical calculation of  $\sigma$  (especially the maximum value of  $\sigma = \sigma_1$ ) is widely used as a tool for the characterisation of chaos in Hamiltonian as well as dissipative systems. The numerical method has been discussed in detail by several authors [20,22].

### 1.5 Importance of deterministic chaos

Before concluding this chapter, we discuss some of the important aspects of the study of chaotic systems as well as some novel ideas that 'deterministic chaos' has brought about. Until recently, it was believed that the lack of predictability in several natural phenomena, such as weather, resulted from the failure to gather and process a sufficient amount of information. Such a viewpoint has received a great blow by the discovery of chaos in simple deterministic systems where the randomness is 'fundamental'; gathering more information does not necessarily make it go away. In other words, the unpredictability cannot be avoided by making the observation more precise. As such, we can say that nature

imposes a fundamental limit on our power of prediction. Lorenz [3] has put this idea elegantly in what he called the 'butterfly effect': that is, even a small disturbance caused by the flapping of a butterfly's wings is sufficient for changing the weather.

But the study of chaotic systems has been encouraging in many other respects. Chaos helps certain common or unifying features to be found in the behaviour of simple models representing many diverse phenomena such as, for example, the chemical reaction, the fluid convection and the biological rhythms [23]. The determinism inherent in chaos implies that many random phenomena are more predictable than had been previously thought. A particularly interesting field of research is to understand the fluid turbulence in terms of the dynamical chaos. This is partly motivated by the complicated fractal structure of the attractors underlying the chaotic flows. It is indeed true that chaotic attractors have been found to exist in some of the fluid convection experiments [24,25]. But an adequate

understanding of the turbulent state is far from complete. This is mainly because turbulence, as we know, necessarily include space-time structures where as chaos can only be considered as a 'turbulence in time'. And it is clear that the complex spatial patterns cannot be usefully described by the usual strange attractors in a single state space. Perhaps, the experience with the low dimensional chaotic attractors can serve as a guide to a more advanced picture of the real world turbulence.

## II. MATHEMATICAL MODELS OF CHAOTIC DYNAMICS

In spite of the recent advances in nonlinear dynamics, our understanding of the properties of even the simplest of nonlinear systems is still rudimentary. Whatever progress we have achieved today, comes mostly from the study of various mathematical models of chaotic phenomena. We will present here the most important ones among them namely, the logistic map, the Henon map, the Lorenz model and the Duffing Oscillator. Each of these models represent a particular class of systems. After a brief discussion of these models, we will concentrate on the logistic map to study in detail the period doubling route to chaos and the 'universal' properties associated with it. We then introduce a new two dimensional noninvertible map of the unit square analogous to the logistic map, and investigate its properties in detail in the subsequent chapters.

### 2.1 One dimensional mappings: The logistic map

Logistic map is a first order nonlinear difference equation of the form

$$X_{t+1} = f_{\lambda}(X_t) \equiv 4\lambda X_t(1 - X_t) \quad (17)$$

and is a representative of a whole family of maps known as 'the quadratic family'. Here  $\lambda$  is a control parameter which can be thought to represent the interaction of the system with the surroundings. We will see below that the asymptotic behaviour of the system depends crucially on the value of  $\lambda$ .

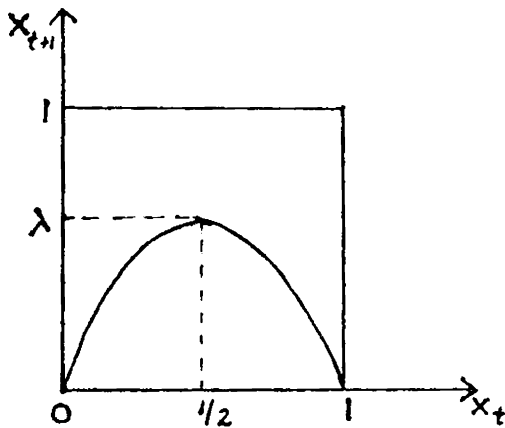


Fig.4 The logistic map on the unit interval

The map is illustrated in fig. 4. It is not difficult to see that this equation possesses non-trivial dynamical behaviour only when  $X_t$  remains in the interval  $0 < X_t < 1$ ; if  $X_t$  ever exceeds unity, subsequent iterations diverge towards  $-\infty$ . Furthermore, we see from fig. 4 that the function  $f(X_t)$  attains a maximum value of  $\lambda$  at  $X_t = 1/2$ . Therefore

the map is interesting only when  $\lambda < 1$  and for  $\lambda \in [0,1]$ , equation (17) acts as a continuous map of the interval  $[0,1]$  into itself. We often say that the logistic map is a 'one hump' map of the unit interval on the real line or a 'unimodal' map. A typical property of the map is the non-invertibility, that is,  $X_{t+1}$  is uniquely determined by  $X_t$  whereas the reverse is not true as can easily be seen from the figure.

Now, there are countless situations where the first order nonlinear difference equations, such as the logistic map, arises as a natural model of system behaviour [2,27]. A typical example is in population biology where it is used to simulate the growth of a population in a closed area. The magnitude of the population in generation  $t+1$ , say  $X_{t+1}$ , is related to the magnitude of the population in the preceding generation  $t$ ,  $X_t$ : such a relationship can be expressed in the above form. They can also arise in an entirely different context as well, namely, as a Poincaré map of a highly dissipative flow. We know that the Poincaré section of a three dimensional flow is, in general, a two

dimensional surface. But if the flow has a large dissipation, resulting in a rapid contraction of areas, its Poincaré section can practically be considered to be a set of points distributed along a curve. In this case, one defines a coordinate  $X$  for each point on the curve and studies how  $X$  varies with time. In other words, the problem has now been reduced to a one dimensional noninvertible map of the form

$$X_{t+1} = f(X_t) \quad (18)$$

and is often called a 'first return map'.

Now, logistic map is only a particular form of equation (18) and the chaotic behaviour is not tied to the special form of the logistic map. Feigenbaum [12,13,28] has shown that the route to chaos which is found in the logistic map, the 'Feigenbaum route', occurs in all one hump maps of an interval on the real line. He found that the scaling behaviour at the transition to chaos is governed by universal constants, the Feigenbaum



constants  $\alpha$  and  $\delta$ , whose values depend only on the order of the maximum, which is 'quadratic' in the case of the logistic map.

Apart from this universal scaling behaviour, the logistic map shows another interesting property which is also universal for all one hump maps. This is known as the Sarkovskii ordering which refers to the ordering of the infinite number of periodic windows of the map along the parameter axis and is discussed in detail in the next chapter.

Two other equivalent forms of the logistic map often found in the literature [14,29] are

$$X_{t+1} = 1 - \lambda X_t^2$$

and  $X_{t+1} = \lambda - X_t^2$ .

The universal scaling properties of the quadratic maps are reviewed in sec. 2.3.

## 2.2 Higher dimensional models

### The Henon Map

Probably one of the simplest mathematical models yielding a strange attractor is given by the

the following two dimensional invertible map of the plane:

$$\begin{aligned} X_{t+1} &= 1 + Y_t - a X_t^2 \\ Y_{t+1} &= b X_t \end{aligned} \tag{19}$$

This map was invented by Henon in 1976 [26]. Because of the extreme elegance and analytical simplicity, the Henon map has been the subject of a wide variety of further investigations [30-34] and has also been used as a model problem in, for example, the development of new ideas regarding the fractal structure of strange attractors [35].

The map contains two parameters  $a$  and  $b$ . It can be easily seen that the Jacobian determinant of the map is  $-b$ . Therefore the map is conservative for  $|b| = 1$  and dissipative for  $|b| < 1$ . Note that in the limit of extreme dissipation ( $b \rightarrow 0$ ), the map reduces to the one dimensional quadratic map. In order to study the bifurcations in the system, the parameter  $b$  is usually adjusted to give a moderate dissipation. In most of the studies  $b$  is fixed at 0.3, and as the parameter  $a$  is varied, the map follows the period doubling route to chaos. More

interestingly, it can be shown that at the transition to chaos it obeys the universal behaviour of Feigenbaum. This is basically because for  $|b| \ll 1$ , the map becomes effectively one dimensional in the renormalisation limit [36]. The most important aspect of the Henon map is that for  $a = 1.4$  and  $b = 0.3$ , the map generates a strange attractor [26], now well known as the 'Henon attractor'. This is one of the few strange attractors where the self similar structure can be seen very clearly. Eventhough the Henon map has undergone extensive study since its introduction, certain domains of parameter space are yet to be analysed completely.

### The Lorenz and Duffings systems

Compared to the discrete nonlinear mappings, studies on chaotic behaviour using systems of differential equations are relatively few. So far most of the studies have been confined to two groups of systems. The first group includes autonomous differential equations with three or more variables. These are obtained either by truncating the well known

Navier - Stokes equations [3,37] or by artificial construction [38]. The second group consists of nonlinear oscillators driven by external periodic force [39]. It has also been shown that these two groups are related since periodically driven systems can be written as systems of autonomous differential equations by introducing new variables [40]. We will present here two examples, one from each group.

In 1963, Lorenz [3] studied a set of three ordinary differential equations which could model some of the unpredictable behaviour which we normally associate with the weather. The equations were derived from a model of fluid convection. They are:

$$\begin{aligned}\frac{dX}{dt} &= \sigma (Y - X) \\ \frac{dY}{dt} &= rX - Y - XZ \\ \frac{dz}{dt} &= XY - bz\end{aligned}\tag{20}$$

where  $\sigma$ ,  $r$  and  $b$  are three real positive parameters. Roughly,  $X$  measures the rate of convective overturning,  $Y$  the horizontal temperature variation

and  $z$  the vertical temperature variation. Since then, the Lorenz equations have been shown to arise in several other experimental situations also. For example, Haken [41] has derived them from a problem of irregular spiking in lasers.

The Lorenz system shows several types of bifurcations and chaotic behaviour depending on the parameter values. In his original paper, Lorenz put the parameter values as  $\sigma = 10$ ,  $b = 8/3$  and examined the behaviour of the system for several values of  $r$  in the range  $0 < r < \infty$ . He found that for wide ranges of parameter values, the approximate solutions, calculated on a computer, were extremely complicated. The value  $r = 28$  was carefully studied by Lorenz and he showed that the trajectory continues to wind around and around, without ever settling down to either periodic or stationary behaviour. The corresponding attractor, known as the 'Lorenz attractor', has been shown in the previous chapter. Incidentally, this is the first strange attractor observed numerically.

The Lorenz model possesses some other elegant properties also. For example, the equations

have a natural symmetry with respect to the change of  $X$  and  $Y$  variables into  $-X$  and  $-Y$  respectively. That is, the equations are unchanged even if  $(X, Y, Z) \longrightarrow (-X, -Y, Z)$ . Also, the  $Z$ -axis,  $X = Y = 0$ , is invariant. All trajectories which start on the  $Z$ -axis, remain on it and tend towards the origin. Since Lorenz, the model has been analysed extensively by several authors. A more or less complete account of these studies has been given by Sparrow [42].

The Duffing oscillator originally arose as a model to describe the hardening spring effect observed in many mechanical systems [43]. Since then, this model has become a common example of nonlinear oscillation problems. The equation can be written in the form

$$\ddot{X} + \delta \dot{X} - \beta X + X^3 = \gamma \cos wt \quad (21)$$

where  $\delta$  is the damping parameter and the right hand side provides the periodic forcing.

It can also be written as an autonomous flow in three variables. Usually,  $\delta$  and  $w$  are taken

as fixed positive quantities and the system is examined by varying  $\gamma$ . As  $\gamma$  is increased, the periodic orbits of the flow double their periods repeatedly and accumulate at a point at which transition from periodic to apparently chaotic nonperiodic motion takes place. These period doubling bifurcations have been studied extensively and are shown to obey the universal behaviour of Feigenbaum. Moreover, for relatively wide sets of parameter values, strange attractors have been observed numerically. It is also seen that these strange attractors can coexist with simple periodic motions in thin bands within the chaotic region. For a detailed discussion of the Duffing oscillator, see the excellent monograph by Guckenheimer and Holmes [43].

### 2.3 One dimensional maps and universality

One dimensional maps are simple enough to be accessible to certain analytical tools and are not very time consuming in numerical study. At the same time they are rich enough to show many of the scaling and universal properties of chaotic

transitions observed in higher dimensional systems. In particular, we shall treat in some detail the period doubling and universal properties of one dimensional quadratic maps. For concreteness we shall choose the logistic map, equation (17).

We are mainly interested in the behaviour of the system after many iterations for a given value of  $\lambda \in [0,1]$ . Note that if the initial condition  $X_0 = 0$ , then all the remaining iterates are zero. We say that zero is a trivial fixed point of equation (17). In general, a point  $X^*$  is said to be a fixed point of a function  $f(x)$  if it satisfies the equation  $X^* = f(X^*)$ . Fixed points play a very important role in the theory of mappings because they force a definite structure for the trajectories in their neighbourhood. A 'cycle of period-n' or an 'n-cycle' of a function  $f(x)$  is a finite sequence of points  $X_0, \dots, X_{n-1}$  such that

$$X_1 = f(X_0), \dots, X_{n-1} = f(X_{n-2}), X_0 = f(X_{n-1}).$$

In other words, it is a periodic trajectory, which comes back to the same point after n iterations. Every point  $X_j$  of the cycle satisfies  $X_j = f^n(X_j)$



and is therefore a fixed point of the function  $f^n$ . A fixed point of  $f$  is simply a cycle of period 1. Thus, there is no fundamental difference between fixed points and cycles.

Applying the fixed point condition to the logistic map,

$$X^* = 4\lambda X^* (1-X^*) \quad (22)$$

We get two fixed points

$$X^* = 0, \quad X^* = 1 - 1/4\lambda. \quad (23)$$

For all values of  $\lambda$  in the range  $0 \leq \lambda < 1/4$  the iterates will eventually be attracted towards  $X=0$ . That is, zero is a stable fixed point for  $\lambda < 1/4$ . As  $\lambda$  crosses  $1/4$ ,  $X=0$  becomes unstable and ceases to be attracting where as the other fixed point, namely,  $X_0^* = 1 - 1/4\lambda$  becomes stable simultaneously. The reason for this is that the slope of  $f(x)$  at  $X = 0$  becomes greater than 1 when  $\lambda$  crosses  $1/4$ . One can easily show that a fixed point  $X^*$  of a function  $f(x)$  is stable only if  $|f'(x^*)| < 1$  where  $f'(x) = \frac{df}{dx}$ . As  $\lambda$  increases beyond  $3/4$ ,  $|f'(X_0^*)| > 1$  making  $X_0^*$  also unstable. At  $\lambda = 3/4$ ,

instead of having a stable cycle of period 1 corresponding to one fixed point, the system now has a stable cycle of period 2. In other words, a period doubling bifurcation takes place at this value of  $\lambda$ . This process repeats and infinitum as  $\lambda$  goes on increasing and finally at a critical value of the parameter, the iterates become apparently chaotic. The mechanism of period doubling can be clearly understood using a graphical analysis [28]. At this stage, it is interesting to note a basic property of all unimodal maps of an interval. It has been explicitly shown by Guckenheimer et.al [44] that for maps with one critical point there can at most be one stable attractor to which almost all initial conditions (excepting a set of measure zero) will be attracted asymptotically. This implies that if there exists a stable periodic cycle for the logistic map, almost all initial conditions in the interval  $[0,1]$  will eventually be attracted towards it. When the stable periodic cycles of the map are plotted as a function of the parameter  $\lambda$ , we get a graph as shown in fig.5.

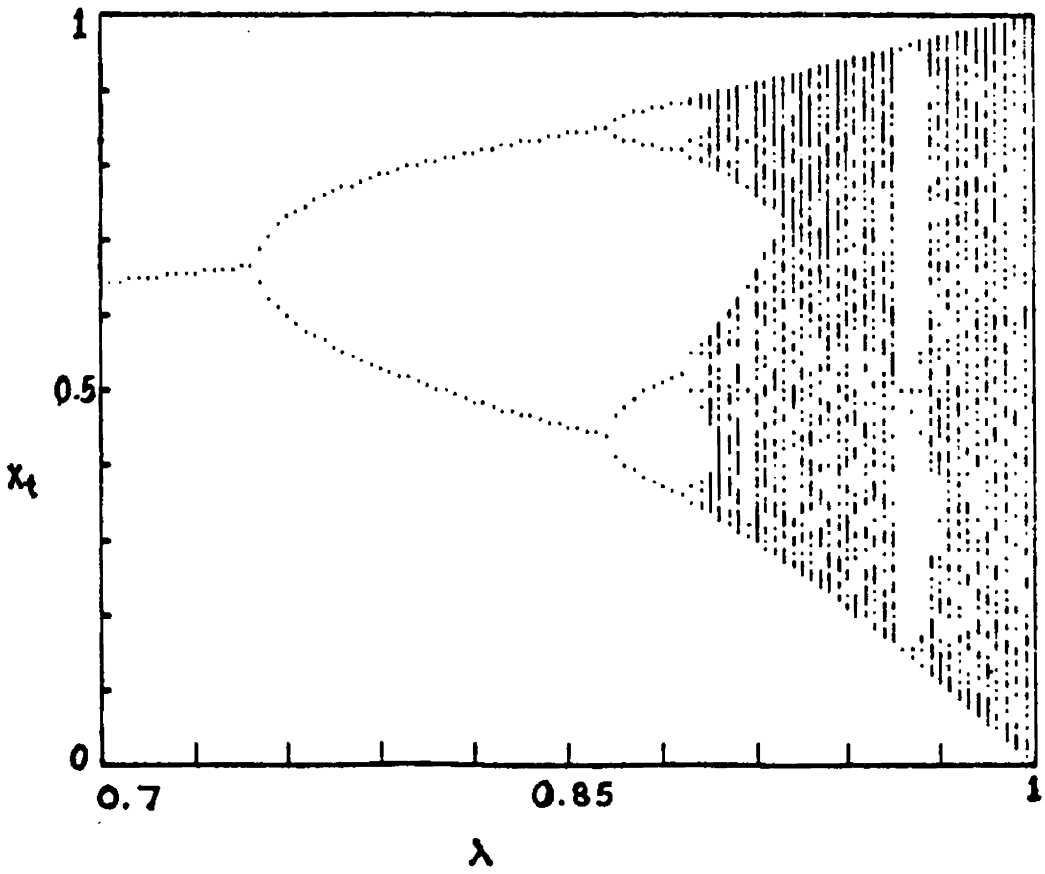


Fig. 5 The Bifurcation structure of the logistic map

This is known as the 'bifurcation structure' of the map and represents the period doubling transition to chaos.

The period doubling route was analysed in detail by Feigenbaum [12,13] by applying the renormalisation techniques. He discovered that the transition to chaos is characterised by two universal constants  $\alpha$  and  $\delta$  which are independent of the particular form of the function. Since then this route has come to be known as the 'Feigenbaum scenario'. As a first step towards the universality theory, we note that (a) for  $\lambda_{n-1} < \lambda < \lambda_n$  there exists a stable  $2^{n-1}$ -cycle with elements  $x_1^* \dots x_{2^{n-1}}^*$  which is characterised by

$$\left| \frac{d}{dx_1} f^{2^{n-1}}(x_1^*) \right| \equiv \left| \prod_{i=1}^{2^{n-1}} f'(x_i^*) \right| < 1 \quad (24)$$

and (b) at  $\lambda_n$  all points of the  $2^{n-1}$ -cycle become unstable simultaneously via pitchfork bifurcation in

$$f^{2^n} = f^{2^{n-1}} \circ f^{2^{n-1}} \quad (25)$$

which lead to a new stable cycle of period  $2^n$  for  $\lambda_n < \lambda < \lambda_{n+1}$ . The crucial point here is that the

mechanism that  $f^{2^{n-1}}$  uses to period double at  $\lambda_n$  is the same one that  $f^{2^n}$  will use to double at  $\lambda_{n+1}$ . This conclusion is the starting point of universality because it connects the mechanism of subsequent bifurcations to a general law of functional composition.

A periodic cycle  $X_i^*$  of period  $2^n$  is said to be superstable if

$$\frac{d}{dX_1^*} f^{2^n}(X_1^*) = \pi_i f^1(X_1^*) = 0 \quad (26)$$

which implies that it always contains the critical point of the map ( $X_1^* = 1/2$ ) as the cycle element since this is the only point where  $f^1(X) = 0$ .

Consider a superstable cycle of period  $2^{n-1}$ . If  $d_n$  is the distance between the cycle element  $X^* = 1/2$  and its nearest neighbour given by  $f^{2^{n-1}}(1/2)$ , then

$$d_n = f^{2^{n-1}}(1/2) - 1/2 \quad (27)$$

Performing a coordinate transformation to displace  $X = 1/2$  to  $X = 0$ , we get

$$d_n = f^{2^{n-1}}(0) \quad (28)$$

We can show numerically that the distance  $d_n$  scales

down by an approximately constant factor, say  $\alpha$ , between successive superstable cycles. In other words,

$$\frac{d_n}{d_{n+1}} = -\alpha \quad (29)$$

This implies that

$$\lim_{n \rightarrow \infty} (-\alpha)^n d_{n+1} = d_1 \quad (30)$$

or, 
$$\lim_{n \rightarrow \infty} (-\alpha)^n f^{2^n}(0) = d_1 \quad (31)$$

which shows that the sequence of scaled iterates converge to a limiting function, say  $g_1(x)$ , given by

$$\lim_{n \rightarrow \infty} (-\alpha)^n f^{2^n} \left( \frac{x}{(-\alpha)^n} \right) = g_1(x) \quad (32)$$

Similarly we can introduce a whole family of functions  $g_i(x)$  corresponding to each of the superstable cycles and we can show that any two successive functions are related by a 'doubling transformation'

T:

$$g_{i-1}(x) = (-\alpha) g_i \left[ g_i \left( \frac{-x}{\alpha} \right) \right] \equiv T g_i(x) \quad (33)$$

Taking the limit  $i \rightarrow \infty$ , the function

$$g(X) = \lim_{i \rightarrow \infty} g_i(X) \quad (34)$$

becomes a fixed point of the doubling operator  $T$ :

$$g(X) = T g(X) = -\alpha g \left[ g \left( \frac{-X}{\alpha} \right) \right] \quad (35)$$

This equation determines  $\alpha$  universally by

$$g(0) = -\alpha g [g(0)] \quad (36)$$

A unique solution for this equation can be obtained if we specify the nature of the maximum of  $g(X)$  at  $X = 0$ . Thus, the value of  $\alpha$  is same for all quadratic functions and can be shown to be equal to

$$\alpha = 2.502907875 \dots$$

This establishes the universality of  $\alpha$ .

Let us now consider the scaling along the parameter axis. From figure 5, one can easily see that the points  $\lambda_n$  at which bifurcations take place converge geometrically to a critical point  $\lambda_\infty$  whose value for the logistic map is given by 0.8924864 ... This is exactly the way in which the successive superstable values of the parameter, say

$\Lambda_n$ , also converge. If we write the bifurcation ratio as  $\delta$ , the scaling relation can be written as

$$\Lambda_n - \Lambda_\infty \propto \delta^{-n}. \quad (37)$$

The values  $\Lambda_n$  are determined by the condition that  $X = 1/2$  is an element of the supercycle, that is,  $X = 1/2$  is a fixed point of  $f_{\Lambda_n}^{2^n}(X)$  :

$$f_{\Lambda_n}^{2^n}(1/2) = 1/2 \quad (38)$$

which after translation by  $1/2$  becomes

$$f_{\Lambda_n}^{2^n}(0) = 0 \quad (39)$$

Expanding  $f_{\Lambda_n}(X)$  around  $f_{\Lambda_\infty}(X)$ , we get

$$f_{\Lambda}(X) = f_{\Lambda_\infty}(X) + (\Lambda - \Lambda_\infty) \delta f(X) \quad (40)$$

$$\text{where } \delta f(X) = \left. \frac{\partial f_{\Lambda}(X)}{\partial \Lambda} \right|_{\Lambda_\infty} \quad (41)$$

Applying the doubling operator  $T$  to this equation, one can show that  $\delta$  is the only relevant ( $>1$ ) eigen value of the linearised doubling operator and is hence universal. The value of  $\delta$  for quadratic maps has been calculated to be  $\delta = 4.6692016 \dots$



We can summarise the results in the form of two equations, as follows:

- (1) the existence of a universal rescaling coefficient at the transition to chaos

$$\lim_{n \rightarrow \infty} \frac{d_n}{d_{n+1}} = \alpha \quad (42)$$

- and (2) a universal bifurcation ratio at the point of accumulation of period doubling bifurcations

$$\lim_{n \rightarrow \infty} \frac{\lambda_n - \lambda_{n-1}}{\lambda_{n+1} - \lambda_n} = \delta \quad (43)$$

These two numbers determine quantitatively the transition from periodic to chaotic behaviour for a large class of nonlinear systems.

#### 2.4 A 'modulated' logistic map

In this section we introduce a new two dimensional (2D) noninvertible map:

$$\begin{aligned} X_{t+1} &= 4 \lambda_t X_t (1 - X_t) \\ \lambda_{t+1} &= 4 \mu \lambda_t (1 - \lambda_t) \end{aligned} \quad (44)$$

That is, we have considered a situation where the parameter of the logistic map  $\lambda$  at any instant is a

simple nonlinear function of its value at the previous instant. We call it a "modulated" logistic map (MLM) where the role of the control parameter is played by  $\mu$ , which is confined to the interval  $0 \leq \mu \leq 1$ . Note that the map has the following properties analogous to the logistic map:

- (a) it consists of two coupled first order difference equations which map the unit square  $\{x, \lambda \mid 0 \leq x \leq 1, 0 \leq \lambda \leq 1\}$  in  $R^2$  into itself for  $\mu \in [0,1]$  and is continuous over the interval,
- (b) it can be included in a one parameter family of maps and
- (c) as can easily be seen numerically, for a given value of  $\mu$ , there is a unique attractor for the map that 'owns' almost all initial conditions in the unit square. As we see below, this is true even in the chaotic regime where there are infinitely many different periodic orbits and an uncountable number of asymptotically aperiodic orbits. Whether the attractor is periodic or chaotic is determined by the value of  $\mu$ .

Now, there are several experimental situations where the parameter is made time dependant and this time dependance has been shown to induce dramatic changes in the behaviour of the system. For example, during the last few years, there has been an increased interest in the study of different kinds of laser systems by modulating one of its physical parameters [45] and it has been shown that the output can be periodic as well as chaotic depending on the strength of the modulation [46].

Moreover, it has recently been suggested by Ruelle [47] that time evolutions with 'adiabatically fluctuating parameters' (AFPs) may be useful in understanding the chaotic behaviour in some of the systems currently under investigation such as, for example, the pulsating variable stars and EEGs. What Ruelle recommends is the study of evolution of the form

$$X_{t+1} = f (X_t, \lambda (t)) \quad (45)$$

for discrete time. He further proposes that the evolution of  $\lambda$  might itself be determined by a

dynamical system, as in our case. But, instead of assuming a slow variation for  $\lambda$  compared to  $X$ , we choose the same time scale for  $X$  and  $\lambda$ . We now investigate in detail the onset and characterisation of chaos in this model.

### III BIFURCATIONS AND UNIVERSALITY IN THE MODULATED LOGISTIC MAP

This chapter is devoted to the study of onset of chaos in MLM introduced in the previous chapter and the universal properties associated with it. It is organised as follows. In Sec. 3.1, the map is shown to follow the period doubling route to chaos. Some novel features of the bifurcation structure are also discussed. Sec. 3.2 is devoted to a detailed study of the universal scaling behaviour of the map at the transition to chaos. Using approximate renormalisation methods, it is shown that the map comes under the universality class of Feigenbaum. Finally, in Sec. 3.3 we give numerical evidence for the existence of Sarkovskii ordering in MLM. The importance of this result has also been discussed in detail.

#### 3.1 Bifurcation structure and linear stability analysis

It is known that  $\lambda_t$  undergoes a cascade of period doubling bifurcations as  $\mu$  is increased, and turns chaotic at a critical value of the parameter,  $\mu_\infty$ . We now concentrate on the values of

$X_t$ . Since  $\lambda_t$  has a single attracting fixed point for  $0 < \mu < 0.75$ , it is obvious that  $X_t$  will also have the same behaviour. For many values of  $\mu > 0.75$ ,  $\lambda_t$  will have stable cycles whose period depends on the value of  $\mu$ . So, at first sight, one might expect that the corresponding  $X_t$  values will vary randomly without being attracted to any stable cycle. However, as we see below, this is not true. It is seen that  $X_t$  also undergoes a cascade of period doubling bifurcations and turns chaotic at exactly the same parameter value  $\mu_\infty$  at which the logistic map turns chaotic. But the bifurcation structure of  $X_t$  has some novel features compared to that of  $\lambda_t$ .

To compute the bifurcation structure, we start from a parameter value  $\mu = 0.7$  and increase it by steps of 0.01, always using an initial condition for  $(X_t, \lambda_t)$  in the interval  $[0,1]$ , say  $(0.3, 0.3)$ . The important asymptotic values of  $\lambda_t$ ,  $X_t$  and the corresponding values of  $\mu$  are collected in table I.

Plotting these values against  $\mu$ , we get the 3D bifurcation diagram of MLM. But in order to study the behaviour of  $X_t$ , it is useful to take a 2D projection of the diagram in the  $(X_t, \mu)$  plane, which is shown in fig. 6.

Table I: Asymptotic values of  $\lambda_t$  and  $x_t$

$\mu$	$\lambda_t$	$x_t$
0.7	0.6428571	0.6111111
0.74	0.6621622	0.6224488
0.75	0.6683250	0.6202936
	0.6649998	0.6296404
0.78	0.5475750	0.7489202
	0.7729381	0.4118614
0.8	0.5130444	0.7539450
	0.7994550	0.3807031
0.84	0.4623756	0.7534620
	0.8352432	0.3435580
		0.7534756
		0.3435452
0.85	0.4519632	0.7340323
	0.8421544	0.3529470
		0.7693097
		0.3208439
0.87	0.3950656	0.8688380
	0.8316804	0.1800840
	0.4871584	0.4912024
	0.8694256	0.4870072
0.89	0.3488245	0.8894232
	0.8086390	0.1372268
	0.5508806	0.3829568
	0.8807835	0.5206940
	0.3738138	0.8792732
	0.8333148	0.1587240
	0.4944891	0.4450920
	0.8898920	0.4885256

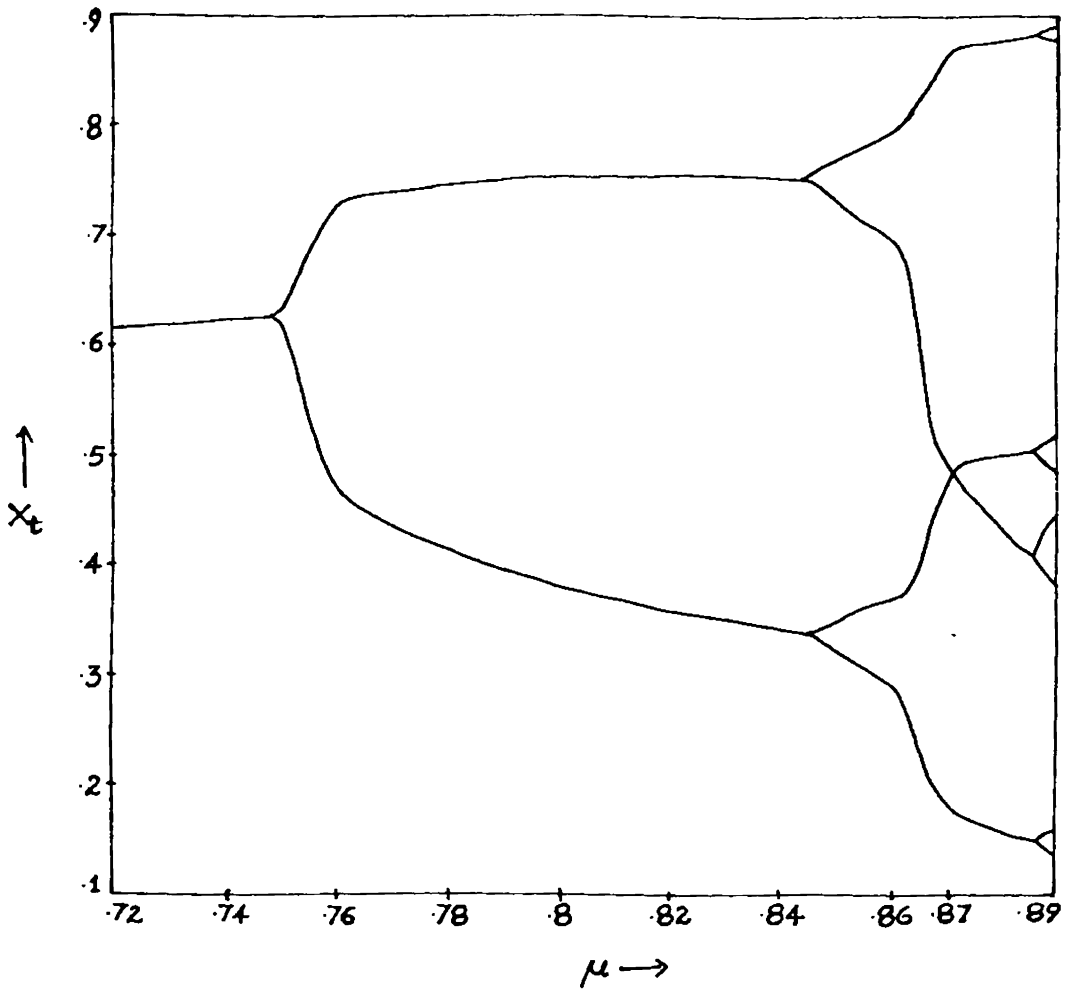


Fig. 6 Bifurcation structure of MLM projected in the  $(X_t, \mu)$  plane. The branches cross over each other in the 4-cycle region resulting in a complete modification of the structure.



It is clear that even from the first bifurcation onwards the structure is quite different from that of the logistic map (shown in fig. 5). One novel aspect of the diagram is that the inner bifurcation branches cross over each other in the 4-cycle region. Although the branches appear to cut each other, it is not so because we are only considering the projection of the 3D diagram in a 2D plane. The crossing over of the bifurcation branches is the result of a significant change in the asymptotic behaviour of the system from the normal one, in a small range of the parameter, say  $\mu=0.86$  to  $0.87$ . In this small range, the branches appear to be very steep indicating that the asymptotic behaviour of the system in this region is very sensitive to small changes in the parameter values. To have a closer look at this region, we calculated the orbits in that range by increasing  $\mu$  in steps of  $0.002$ , and is shown in fig. 7. From the figure we see that as  $\mu$  is increased from  $0.861$  to  $0.865$ , the lower branch shoots up and the upper branch sharply comes down to eventually cross each other at some value around  $\mu = 0.87$ .

Another important observation is that the bifurcations occur earlier than in the case of the

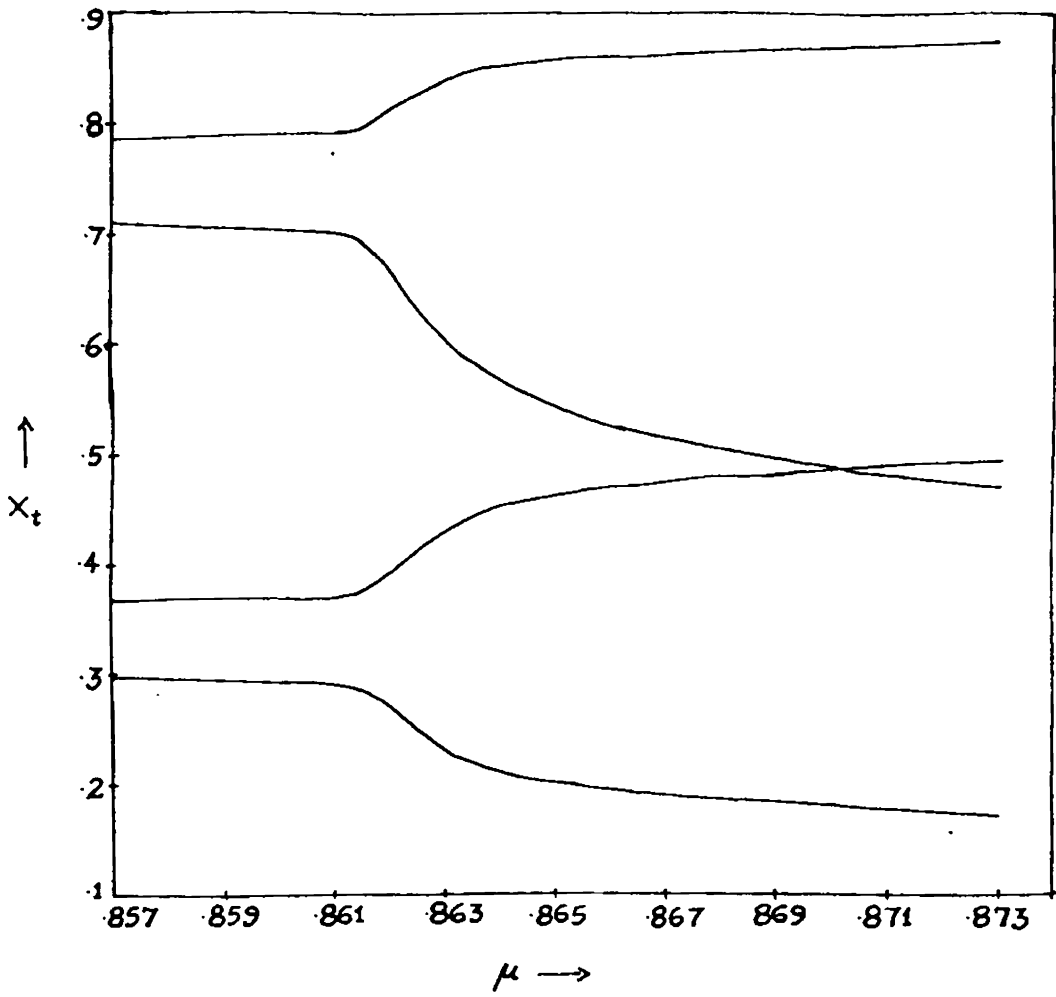


Fig. 7 The 4-cycle region of the figure 6 is shown magnified. The inner branches cross over at a value of  $\mu$  around 0.87.

logistic map from the second bifurcation onwards. This is clearly evident in the case of 2-cycle (see table I or fig.6) which becomes unstable at  $\mu = 0.86225$  for the logistic map, whereas, for the MLM it is somewhere around  $\mu = 0.845$  with the value of the parameter  $\lambda$  still lower. The difference becomes less pronounced as we go to the higher and higher bifurcations.

Finally, we note a peculiar aspect of the bifurcation diagram. It can easily be seen that fig. 6 lacks the symmetry of the bifurcation structure of the logistic map. There is a marked difference in the bifurcations between the upper and lower arms of our bifurcation tree. All the bifurcations of the upper branch appear to be asymmetric where as that of the lower branch are somewhat symmetric.

Now, the analysis of bifurcation structure by introducing a time dependance to the parameter has been a subject matter for the last few years and it is known that this time dependance can induce dramatic changes in the bifurcation diagram [48].

Kapral and Mandel [49] studied the bifurcation structure of a nonautonomous quadratic map in which the control parameter is assumed to vary linearly in time, and showed that this time dependence delayed the onset of bifurcations in the system . Our result is exactly opposite to the one obtained by them and implies that linear and nonlinear variations of the parameter can have entirely different effect on the asymptotic behaviour of the system.

The crossing of the bifurcation branches in the 4-cycle region also has some interesting consequences. It is known that the ordering of the iterates for any stable period obey certain allowed sequences called the MSS sequences [50] and this ordering is unchanged throughout the entire stability zone. But in fig. 6, this is no longer satisfied, as the ordering is necessarily changed when the bifurcation branches cross over. Moreover, the subsequent band structure is also modified because of the crossing. For example, though the 8-cycle region in fig. 6 appear similar to that of the logistic map, it is not, because the inner branches are interchanged. The change in the band

structure is evident from fig. 8 where we have shown the complete bifurcation diagram of MLM. To summarise, the bifurcation structure of the logistic map is modified qualitatively as well as quantitatively by introducing a specific nonlinear variation for the parameter.

We now try to understand some of the results obtained above by determining the fixed points of the map analytically and then performing a linear stability analysis [51,36]. Taking  $(X^*, \lambda^*)$  as the fixed point of MLM, we get:

$$X^* = [(3\mu-1)/(4\mu-1)], \quad (46)$$

$$\text{and } \lambda^* = (4\mu-1)/4\mu \quad (47)$$

apart from the trivial solution  $(X^*, \lambda^*) = (0,0)$ . It is evident that, for  $0 < \mu < 1/4$ ,  $(0,0)$  is the only stable fixed point of MLM. As  $\mu$  increases beyond  $1/4$ ,  $\lambda^*$  becomes stable whereas  $X^*$  does so only at a higher value of  $\mu$ , say  $\mu'$ . The value of  $\mu'$  is determined by the condition

$$(4\mu'-1)/4\mu' = 1/4 \quad (48)$$

which gives  $\mu' = 1/3$ .

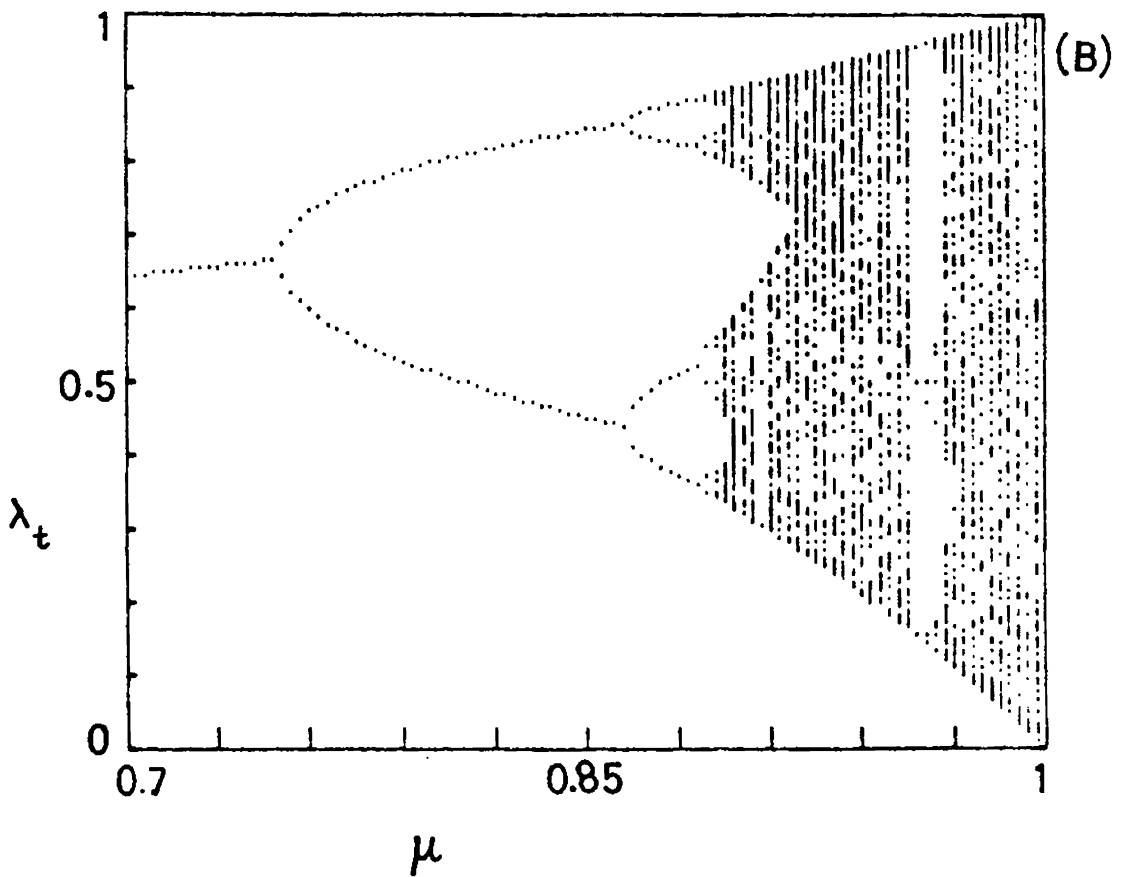
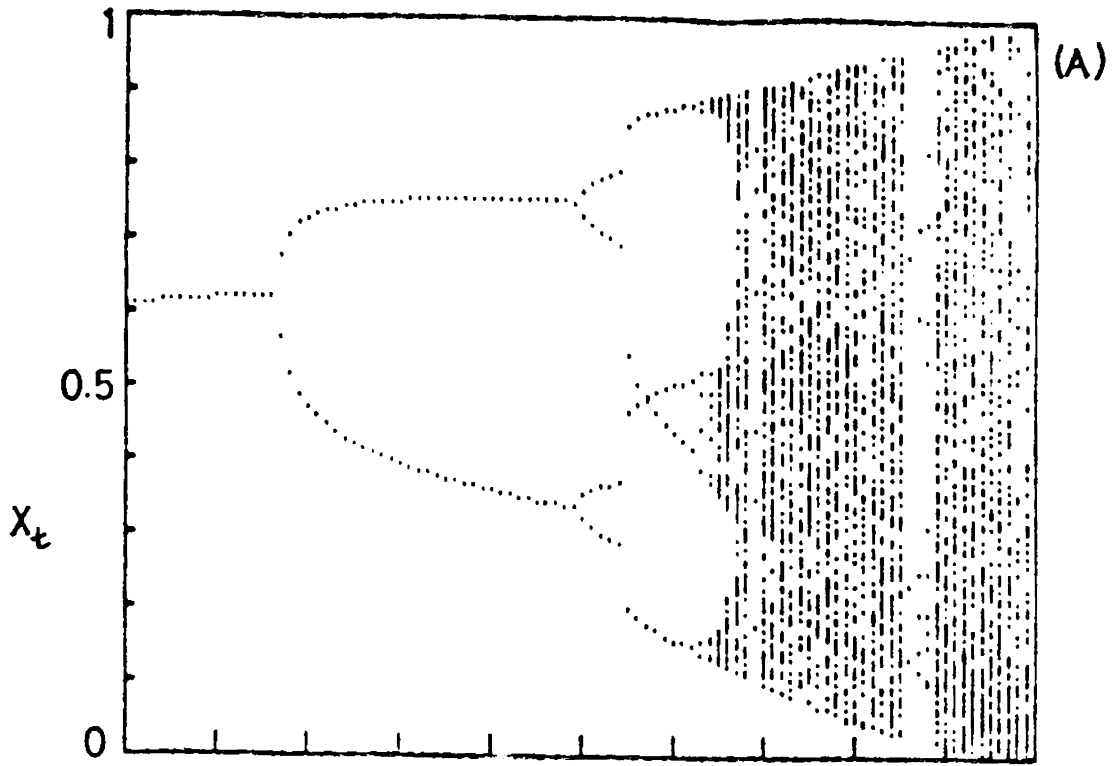


Fig. 8 Projection of the 3D bifurcation diagram of MLM onto (A)  $(X_t, \mu)$  plane and (B)  $(\lambda_t, \mu)$  plane. Note that the band structure in the  $(X_t, \mu)$  plane is different from that in the  $(\lambda_t, \mu)$  plane.

Therefore, for  $1/4 < \mu < 1/3$ , the stable 1-cycle is given by

$$(X^*, \lambda^*) = (0, (4\mu-1)/4\mu) \quad (49)$$

whereas the nontrivial fixed point given by eqns. (46) and (47) becomes stable in the range  $1/3 < \mu < 3/4$  and at  $\mu = 3/4$ , we have the first bifurcation. Now, what we are really interested is in the region  $\mu > 3/4$ . However, it is impractical to obtain the fixed points analytically beyond the 2-cycle.

The 2-cycle, say  $(X_1^*, \lambda_1^*)$  and  $(X_2^*, \lambda_2^*)$  is defined by the following set of four equations:

$$X_2^* = 4 \lambda_1^* X_1^* (1-X_1^*), \quad (50)$$

$$\lambda_2^* = 4\mu \lambda_1^* (1-\lambda_1^*), \quad (51)$$

$$X_1^* = 4 \lambda_2^* X_2^* (1-X_2^*), \quad (52)$$

$$\lambda_1^* = 4\mu \lambda_2^* (1-\lambda_2^*). \quad (53)$$

Since (46) and (47) constitute a trivial solution of eqns. (50) - (53), we can solve them completely to get:

$$\lambda_1^* = (1/8\mu) (4\mu+1) + (1/8\mu) [(4\mu+1) (4\mu-3)]^{1/2}, \quad (54)$$

$$X_1^* = \frac{(5\mu-1)}{2(4\mu-1)} - \frac{1}{2} \left[ \frac{(5\mu-1)^2}{(4\mu-1)^2} + \frac{8\mu(4\mu-1) (\mu^2-4\mu-1)}{\beta (4\mu+1) (3\mu-1)} \right], \quad (55)$$

$$\lambda_2^* = (1/8\mu)(4\mu+1) - (1/8\mu) [(4\mu+1)(4\mu-3)]^{1/2}, \quad (56)$$

$$X_2^* = \frac{(4\mu-1)(4\mu+1-\mu^2)}{(4\mu+1)(3\mu-1)} - \frac{\beta X_1^*}{2(4\mu-1)} \quad (57)$$

$$\text{where } \beta = (4\mu+1) + [(4\mu+1)(4\mu-3)]^{1/2} \quad (58)$$

From eqns. (54) and (56), we see that the bifurcation branches of the logistic map are exactly symmetric whereas eqns. (55) and (57) suggest that such a symmetry is lacking in the case of  $X^*$ . The asymptotic values  $X_1^*$  and  $X_2^*$  depend on each other resulting in the observed asymmetry of the bifurcation branches. Now, to study the stability of the 2-cycle we consider the Jacobian of MLM:

$$J = \begin{bmatrix} 4\lambda_t(1-2X_t) & 4X_t(1-X_t) \\ 0 & 4\mu(1-2\lambda_t) \end{bmatrix}$$

Taking  $M = \prod_{i=1}^2 J(X_i^*, \lambda_i^*)$ , we have

$$\begin{aligned} \text{Tr } M &= 16\lambda_1^* \lambda_2^* (1-2X_1^*) (1-2X_2^*) \\ &\quad + 16\mu^2 (1-2\lambda_1^*) (1-2\lambda_2^*). \end{aligned} \quad (59)$$

For the 2-cycle to be stable, we have the condition  $|\text{Tr } M| \ll 2$ . Substituting eqns. (54) - (57) in (59), the required  $\mu$  values can be obtained numerically. We see that the 2-cycle becomes stable at  $\mu \sim 0.754$  and becomes unstable at  $\mu \sim 0.858$ , which is in agreement with our numerical result that the second



bifurcation in MLM is earlier than that of the logistic map.

### 3.2 Approximate renormalisation methods and calculation of universal constants

Having obtained the qualitative features of transition to chaos, we now try to get the quantitative measures by calculating the bifurcation ratio and rescaling coefficient. For this, we make use of the approximate renormalisation methods developed by Derrida et.al [50,52] and Helleman [53,54]. Eventhough the two methods are similar in principle, both differ from the original functional group renormalisation theory of Feigenbaum.

#### a) Calculation of $\delta$

The method we use for calculating  $\delta$  is the "eigen value matching renormalisation method" developed by Derrida and Pomeau [52] for two dimensional maps. In fact, it is a generalisation of the "equality of slopes" method of Derrida et.al [50] for one dimensional maps.

The basic principle of the method is as follows: Consider a two dimensional map  $(X,Y) \rightarrow T\mu(X,Y)$ .

For the simplest cycles, say, of periods 1,2,3 and 4, one can in general calculate the cycle elements analytically as functions of the parameter  $\mu$ . One can also linearise the map  $T_\mu^{(n)}$  (which is the  $n^{\text{th}}$  iterate of  $T_\mu$ ) in the neighbourhood of the  $n$ -cycle. This linearised map is a  $2 \times 2$  matrix  $M$ . The eigenvalues  $p_n$  of  $M$  can be expressed as a quadratic equation of the form

$$p_n^2 + 2f_n(\mu) p_n + C(\mu) = 0 \quad (60)$$

Here the function  $f_n(\mu)$  represents the linearisation corresponding to the slope in the ID case and one can in fact show that the  $n$ -cycle is stable only when  $-1 \leq f_n(\mu) \leq 1$ . Now, the basic idea of this renormalisation method is to try to associate at each value of  $\mu$ , a value  $\mu'$  such that  $T_\mu$  looks like  $T_{\mu'}^{(2)}$  locally. An approximate way to do so is to say that the linearisation of  $T_\mu^{(n)}$  around a point of cycle  $n$  is identical to the linearisation of  $T_{\mu'}^{(2n)}$  around a point of cycle  $2n$ .

$$\text{Therefore, } f_n(\mu) = f_{2n}(\mu') \quad (61)$$

This relation provides an approximate value for  $\mu_\infty$  and of  $\delta$ . While  $\mu_\infty$  is obtained as the fixed point of renormalisation(61)

$$f_n(\mu_\infty) = f_{2n}(\mu_\infty), \quad (62)$$

$\delta$  is given by

$$\delta = \left. \frac{d\mu}{d\mu^1} \right|_{\mu_\infty}. \quad (63)$$

The choice of small value of  $n$  constitutes an approximation which can be improved by increasing  $n$ . But even with a first order approximation using  $n=1$  and  $n=2$ , the results agree rather well with numerical values.

We now apply this method to MLM. Linearising the map in the neighbourhood of the  $n$ -cycle, we get a  $2 \times 2$  matrix given by

$$M = \prod_{i=1}^n \begin{bmatrix} 4\lambda_i(1-2X_i) & 4X_i(1-X_i) \\ 0 & 4\mu(1-2\lambda_i) \end{bmatrix} \quad (64)$$

We take a first order approximation considering only cycles of period 1 and 2. The stable 1-cycle of the map is given by

$$(X^*, \lambda^*) = \left( \frac{3\mu-1}{4\mu-1}, \frac{4\mu-1}{4\mu} \right) \quad (65)$$

Evaluating  $M$  at the fixed point  $(X^*, \lambda^*)$  and taking the eigen value equation, we get:

$$p^2 + 2f_1(\mu)p + (8\mu + 2/\mu - 8) = 0, \quad (66)$$

$$\text{where } f_1(\mu) = 2\mu - 1/2\mu. \quad (67)$$

Similarly, evaluating  $M$  at the 2-cycle, we get:

$$f_2(\mu) = \frac{1}{2} (4\mu+1)(4\mu-3) - \frac{4\mu+1}{2\mu^2(4\mu-1)} (A^{1/2} - \mu) - \frac{(4\mu+1)(6\mu-1)\beta}{4\mu^2(4\mu-1)^3} [A^{1/2} - (5\mu-1)] + \frac{(4\mu+1-\mu^2)}{\mu^2(3\mu-1)} (A^{1/2} - 3\mu) - \frac{1}{2}, \quad (68)$$

$$\text{where } A = (5\mu-1)^2 - \frac{8\mu(4\mu-1)^3 (4\mu+1-\mu^2)}{(4\mu+1)(3\mu-1)\beta} \quad (69)$$

It can be easily seen that  $|2 f_n(\mu)|$  is equal to  $|\text{Tr } M|$  evaluated at the  $n$ -cycle, so that the  $n$ -cycle is stable when  $|f_n(\mu)| \leq 1$ . In the first order approximation, we equate the linearisation around the 1-cycle and the 2-cycle. This gives an approximate value of  $\mu_\infty$  which is the fixed point of renormalisation:

$$f_1(\mu_\infty) = f_2(\mu_\infty) \quad (70)$$

From extensive numerical calculation, we obtain  $\mu_\infty = 0.890\dots$ , which is very close to the  $\mu_\infty$  of the logistic map. The bifurcation ratio  $\delta$  is given by

$$\delta = \left. \frac{d\mu}{d\mu'} \right|_{\mu_\infty} \quad (71)$$

Interestingly enough, we obtain  $\delta$  as

$$\delta = 4.4339741\dots, \quad (72)$$

which is in close agreement with Feigenbaum's constant, considering the fact that we are taking a first order approximation. This shows that the MLM obeys the universal behaviour of the quadratic maps at the onset of chaos. A more accurate estimate of  $\delta$  can be obtained by taking the higher orders of approximation.

(b) Calculation of  $\alpha$

We now calculate the rescaling coefficient  $\alpha$  of our system using the renormalisation method of Helleman [53,54]. Since the map is two dimensional, there exist two rescaling coefficients for it. Moreover, the coefficient for the variable  $\lambda$  has to be necessarily  $\alpha$ . Our aim is to calculate the second one, say  $\alpha'$ , for the variable  $X$ . The basic principle of the method is to look for the local behaviour about a periodic orbit of the map by expanding it about a periodic point, upto and including second order Taylor terms in the deviations. After proper scaling and counting  $t$  modulo 2, the quadratic part of the mapping about the periodic orbit becomes identical to the original equation we started with. Since  $\lambda$  is decoupled from  $X$  in MLM, a small variation in  $X$  about a periodic point does not lead to a variation in the  $\lambda$ -cycle.

Let  $(X_t^*, \lambda_t^*)$  be a periodic point of MLM. Taking a small variation  $\Delta X_t$  for  $X_t$  about the periodic orbit, the variational equation for  $X_t$  can be written as

$$\Delta X_{t+1} = 4 \lambda_t^* (1-2X_t^*) \Delta X_t - 4 \lambda_t^* (\Delta X_t)^2 \quad (73)$$

Putting  $t = 2\eta+1$  in (73) and taking a periodic orbit of period 2, denoted by

$$(X_{2\eta}^*, \lambda_{2\eta}^*) \equiv (X_1^*, \lambda_1^*); (X_{2\eta+1}^*, \lambda_{2\eta+1}^*) \equiv (X_2^*, \lambda_2^*)$$

we get

$$\begin{aligned} \Delta X_{2\eta+2} = & 4 \lambda_2^* (1-2X_2^*) (\Delta X_{2\eta+1}) \\ & - 4 \lambda_2^* (\Delta X_{2\eta+1})^2 \end{aligned} \quad (74)$$

Now, putting  $t = 2\eta$  in (73),

$$\begin{aligned} \Delta X_{2\eta+1} = & 4 \lambda_1^* (1-2X_1^*) \Delta X_{2\eta} \\ & - 4 \lambda_1^* (\Delta X_{2\eta})^2 \end{aligned} \quad (75)$$

Putting (75) in (74) and collecting terms upto quadratic in  $(\Delta X_{2\eta})$ , we obtain

$$\begin{aligned} \Delta X_{2\eta+2} = & 4[4 \lambda_1^* \lambda_2^* (1-2X_1^*) (1-2X_2^*)] (\Delta X_{2\eta}) \\ & - 4[16 \lambda_1^{*2} \lambda_2^* (1-2X_1^*)^2 + 4 \lambda_1^* \lambda_2^* (1-2X_2^*)] \\ & (\Delta X_{2\eta})^2 \end{aligned} \quad (76)$$

$$\equiv 4 P_\eta (\Delta X_{2\eta}) - 4 Q_\eta (\Delta X_{2\eta})^2 \quad (77)$$

Now, taking  $Y_{\eta} = \alpha^{\downarrow} (\Delta X_{2\eta})$  (78)

where  $\alpha^{\downarrow} = Q_{\eta}/P_{\eta}$ , we get the 'renormalised' mapping

$$Y_{\eta+1} = 4 P_{\eta} Y_{\eta} (1 - Y_{\eta}) \quad (79)$$

which is identical to the original equation. The rescaling coefficient  $\alpha^{\downarrow}$  is given by

$$\alpha^{\downarrow} = \frac{4 \lambda_1^* (1 - 2X_1^*)^2 + (1 - 2X_2^*)}{(1 - 2X_1^*) (1 - 2X_2^*)} \quad (80)$$

Note that  $\alpha^{\downarrow}$  is determined by the control parameter  $\mu$  since  $X^*$  and  $\lambda^*$  are given in terms of  $\mu$ . Using the expressions for the stable 2-cycle of MLM obtained above in the renormalisation limit  $\mu \rightarrow \infty$ , we get the rescaling coefficient as  $\alpha^{\downarrow} = 2.6545422 \sim \alpha$  as a first order approximation. In other words, both the rescaling coefficients of MLM are same and is equal to  $\alpha$ .

The values of  $\delta$  and  $\alpha$  suggests that our model comes under the universality class of Feigenbaum. This result indicates that an important factor for the realisation of such scaling properties is the confinement of the dynamics to an interval, be it in  $R$  or in  $R^2$ .

### 3.3 Universal ordering of periodic windows

When we analyse closely the bifurcation structure of the logistic map, it becomes clear that there are large number of parameter ranges beyond  $\mu_{\infty}$  at which the behaviour is still periodic. Each of these 'periodic windows' consists of a basic cycle and the subharmonic cascade generated from this basic cycle via period doubling bifurcations. The generation of the basic cycle at a particular value of the parameter  $\mu$  is caused by a tangent bifurcation. In principle, there are infinite number of such periodic windows corresponding to the basic cycles of all integer periods. But in practice, only a few of them corresponding to some prominent periods can be observed numerically. We can now view the parameter range  $(0, \mu_{\infty})$  as the largest periodic window, corresponding to the basic cycle of period one. Interestingly, these infinite number of periodic windows, some large and some unimaginably small, are all arranged along the parameter axis in a specific order. Moreover, this ordering is found to be a characteristic property of unimodal maps depending only on the fact that the map has a unique critical point in



the interval. Recall that the convergence rate  $\delta$  and the scaling factor  $\alpha$  in 1D maps are determined by the analytic form of the map near the maximum. Hence they are called universal 'metric' properties whereas the ordering of periodic cycles is a 'structural' universal property of all unimodal maps.

In fact, this ordering is explained using a rigorous mathematical theorem put forward by Sarkovskii [55,56] in as early as 1964. For a simple and elegant exposition of the theorem, see Devaney [57]. Consider the following ordering of natural numbers known as the Sarkovskii ordering:

$$3 \rightarrow 5 \rightarrow 7 \rightarrow \dots \rightarrow 2 \cdot 3 \rightarrow 2 \cdot 5 \rightarrow \dots \rightarrow 2^2 \cdot 3 \rightarrow 2^2 \cdot 5 \rightarrow \dots \rightarrow 2^n \cdot 3 \rightarrow 2^n \cdot 5 \rightarrow \dots \rightarrow 2^n \dots \rightarrow 2^3 \rightarrow 2^2 \rightarrow 2 \rightarrow 1.$$

It follows from Sarkovskii's theorem that if a continuous map  $f$  of an interval in  $\mathbb{R}$  has a periodic point of prime period  $k$  and if  $k \rightarrow \ell$  in the above ordering, then  $f$  also has a periodic point of period  $\ell$ . In other words, the theorem gives a complete accounting of which periods imply which other periods. Note that the above is a unique ordering of all natural numbers and each number occupies a unique

place in this ordering. The theorem correlates every number to a definite periodic cycle of the corresponding period.

Let us now have a closer look at the theorem taking the logistic map as a specific example. The theorem gives a complete account of the total periodic cycles present at a specified value of  $\mu$ . As we know, at most one among these can be stable and attracting. Alongwith this stable cycle, a large number (may be infinite) of unstable periodic cycles also exist in the interval. These cycles 'own' a set of points in the interval which, although uncountable, will have measure zero. A particularly interesting case arises when the map allows a periodic cycle of period 3 (which need not be stable!) in the interval. The theorem then guarantees that we can, in principle, find initial conditions in the interval leading to periodic cycles of all other integer periods. This is the celebrated result of Li and Yorke [58] that 'period 3 implies chaos' which follows naturally from the Sarkovskii's theorem.

Now, we are interested in the order in which stable periodic cycles arise as the parameter is varied. Suppose we start from a parameter value

at which a stable cycle exists for the map. As  $\mu$  is varied, this cycle becomes unstable, but it will nevertheless remain in the interval as an unstable cycle. Now, the crucial point here is that at every stage (i.e., for every value of  $\mu$ ) the map should obey the Sarkovskii's theorem. In other words, if a periodic cycle of 'basic' or 'prime' period is newly created at a particular  $\mu$  value, it should be in a manner without violating the theorem. This has the important consequence that the order in which stable cycles of different prime periods are arranged along the parameter axis is simply the Sarkovskii ordering! This is indeed what we observe in the bifurcation structure where the basic cycle of period 3 is the last one to become stable as we increase  $\mu$ .

It should be carefully noted that Sarkovskii ordering gives just the ordering of different prime periods (or the periodic windows corresponding to these periods) along the parameter axis. Eventhough the complete ordering of all stable cycles can be derived from Sarkovskii theorem, it says nothing about the observability or measure of these cycles. In practice, only cycles of comparatively low periods will have any finite measure on the parameter axis [2] and their analysis

has gained a lot more attention. For a detailed study of the total number of stable cycles of each period and their arrangement, we need the powerful tool of symbolic dynamics. This has been done for a wide class of unimodal mappings using the so called MSS sequences [59,60] and the arrangement was again found to be universal.

### Sarkovskii ordering in MLM

Our aim here is to show that Sarkovskii ordering exists in the MLM also. We have already shown the existence of cycles of periods  $2^n$  in the parameter range  $0 < \mu < \mu_\infty$ . Now we concentrate on the range  $\mu_\infty < \mu < 1$ . Computing the bifurcation structure of MLM in the chaotic region, we compare it with that of the logistic map.

Consider a small range of the parameter  $0.89 \leq \mu \leq 0.91$ . Computing the asymptotic values of  $X_t$  and  $\lambda_t$  for  $\mu$  in this range, we plot them against  $\mu$  separately (see figs. 9A and 9B). They are the projections of the 3D bifurcation structure of MLM onto the  $(X_t, \mu)$  plane and  $(\lambda_t, \mu)$  plane respectively. Moreover, fig. 9B is just the bifurcation structure of the logistic map for the specified range of the

parameter. In figs. 9A and 9B, we denote by  $\mu^{(n)}$  the value of  $\mu$  at which the  $n$ -cycle becomes stable, by  $\mu'^{(n)}$  at which it becomes unstable and by  $\mu_{\infty}^{(n)}$  at which the 'window' of the basic  $n$ -cycle disappears. Periodic windows with basic periods  $n=12$ ,  $n=10$  and  $n=6$  can clearly be seen in that order. A comparison of figs. 9A and 9B shows that  $\mu^{(n)}$ ,  $\mu'^{(n)}$  and  $\mu_{\infty}^{(n)}$  are exactly the same for both of them. In other words, if  $\lambda_t$  has a stable  $n$ -cycle in a particular interval along the  $\mu$ -axis, then  $X_t$  also has a stable  $n$ -cycle in the same interval.

To confirm this, we have repeated the above procedure for another range of the parameter  $\mu$  from 0.95 to 0.97. The projection of the diagram in the  $(X_t, \mu)$  and  $(\lambda_t, \mu)$  planes are shown in figs. 10A and 10B respectively. From the figures, we see that  $X_t$  and  $\lambda_t$  have a window of basic period 3 for exactly the same range of  $\mu$  values.

The above result has the important consequence that the complete 3D bifurcation diagram of MLM has a stable  $n$ -cycle for the same range of  $\mu$  in which the logistic map has a stable  $n$ -cycle. Now, there are infinite number of periodic cycles in the chaotic region and, as has been already said, most

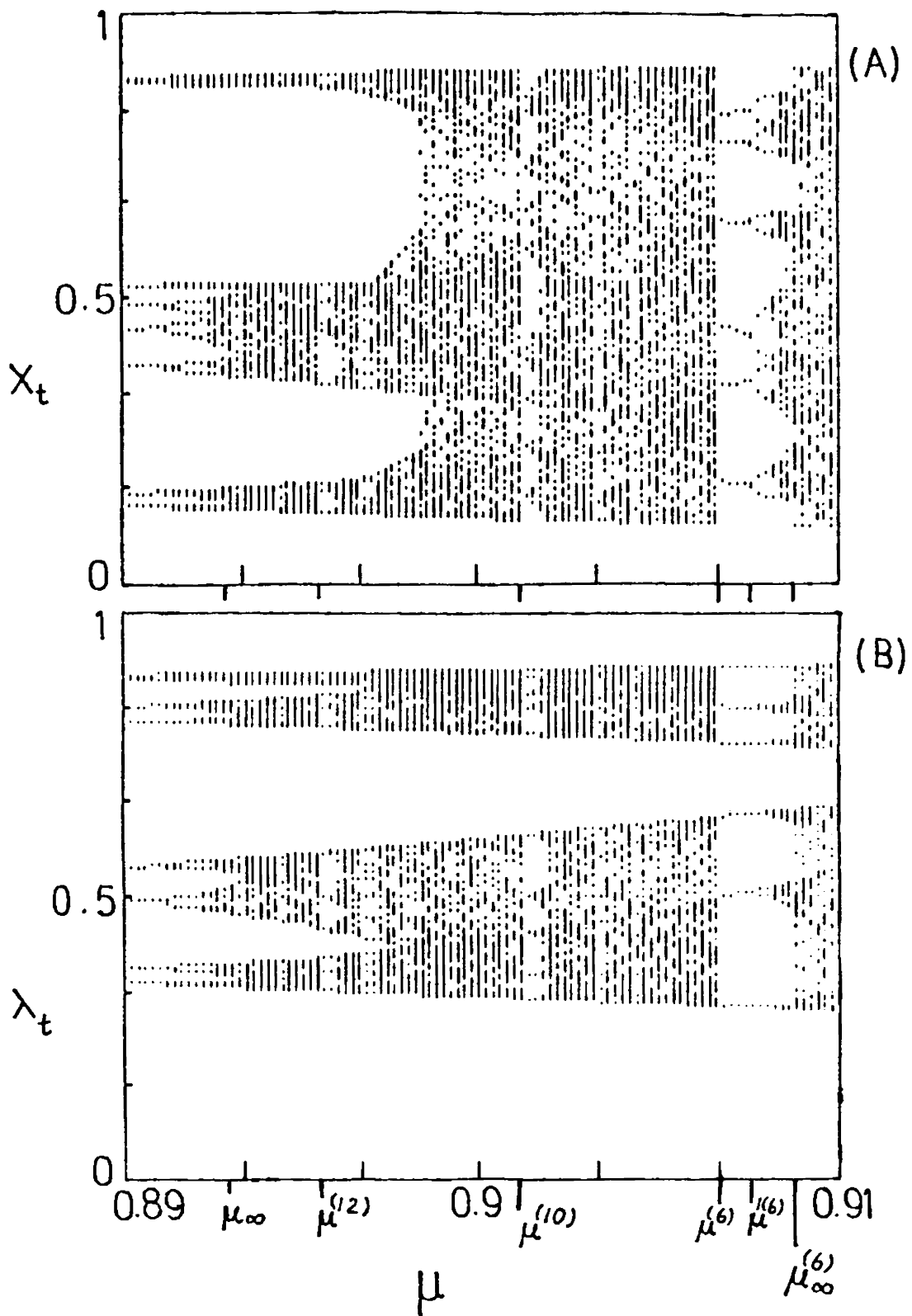


Fig. 9 Bifurcation structure of MLM for the parameter range  $0.89 < \mu < 0.91$  Projected (A) onto the  $(X_t, \mu)$  and (B) onto the  $(\lambda_t, \mu)$  plane.

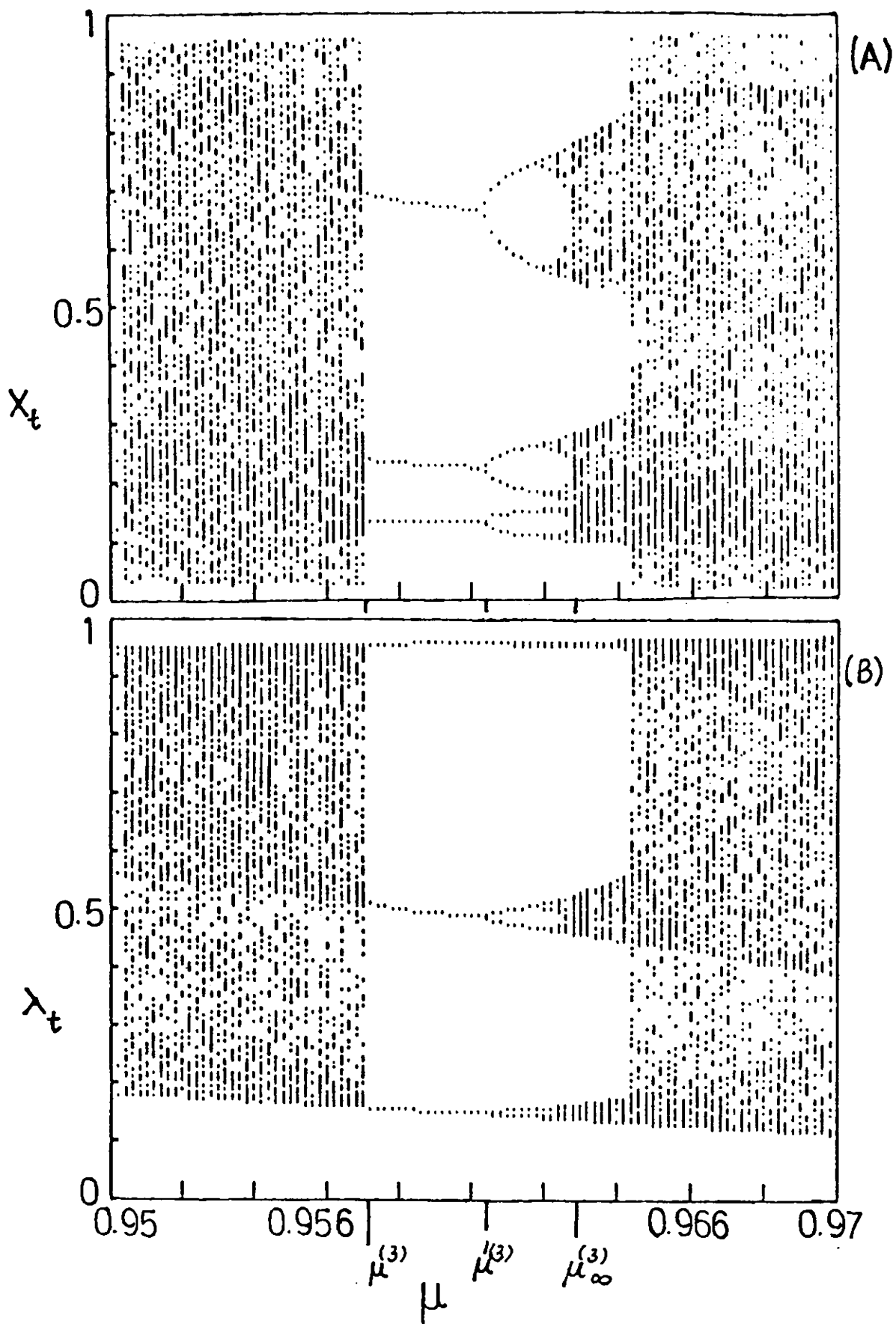


Fig. 10 Bifurcation structure of MLM for the parameter range  $0.95 < \mu < 0.97$  projected (A) onto the  $(X_t, \mu)$  plane and (B) onto the  $(\lambda_t, \mu)$  plane.

of them occupy an extremely narrow window of parameter values. This fact, coupled with the long time it is likely to take for the transients associated with the initial conditions to damp out, implies that in practice the unique cycle is unlikely to be unmasked, excepting the prominent ones. Since the prominent cycles occupy exactly the same interval for the logistic map and the MLM, it is reasonable to expect that the order in which different periodic windows are arranged along the  $\mu$ -axis is the same for both of them. It is also interesting to note that, eventhough the band structure in the  $(X_t, \mu)$  plane is different from that in the  $(\lambda_t, \mu)$  plane, this ordering is left unaffected.

The importance of this result is the following: Sarkovskii's theorem has rigourously been proved only for 1D maps of an interval on the real line [57]. No higher dimensional maps are known to obey Sarkovskii ordering and hence it is widely believed to be only a 1D result. So this turns out to be the first evidence for the existence of Sarkovskii ordering in a 2D map. A possible reason why the Sarkovskii ordering is shown by the MLM is



that it is confined to an interval and has at most one stable cycle for a given value of  $\mu$ . Recall that for 2D maps, in general, more than one attractor, each with its own basin of attraction, can coexist at a given parameter value. For example, Grebogi et.al [61] have shown this for the Henon map, which shares many properties of the 1D quadratic map. It has been proved that Sarkovskii theorem does not hold for the Henon map [57].

Finally, we have only given numerical evidence for the existence of Sarkovskii ordering in a 2D map and not any formal proof of the Sarkovskii theorem in 2D. However, our result suggests that the theorem may hold for continuous maps of an interval on  $\mathbb{R}^2$  as well, and need not strictly be a 1D result.

#### IV. OBSERVATION AND CHARACTERISATION OF CHAOS

In this chapter we analyse the parameter values for which the map is chaotic. To start with, we compute the power spectrum of MLM for one such  $\mu$  value, say 0.98, and compare it with that of the logistic map (see fig. 11). The computation was performed using FFT with  $n = 512$ . The broad band spectrum confirms that  $X_t$  and  $\lambda_t$  evolve in an apparently chaotic manner for  $\mu = 0.98$ . There are such uncountable number of parameter values in the range  $\mu_\infty < \mu < 1$  for which the map is chaotic. In order to study the behaviour of the map at these  $\mu$  values in detail, we make use of certain quantitative measures which have been successfully used to characterise chaos in nonlinear deterministic systems. We mainly concentrate on the Lyapunov exponent (LE) and fractal dimension which are quite general and are applicable to a wide class of problems.

##### 4.1 Lyapunov exponents of the map

There are several analytical as well as numerical works on the LE of the logistic map. For example, the dependence of LE of stable and unstable periodic orbits of the logistic map on the control

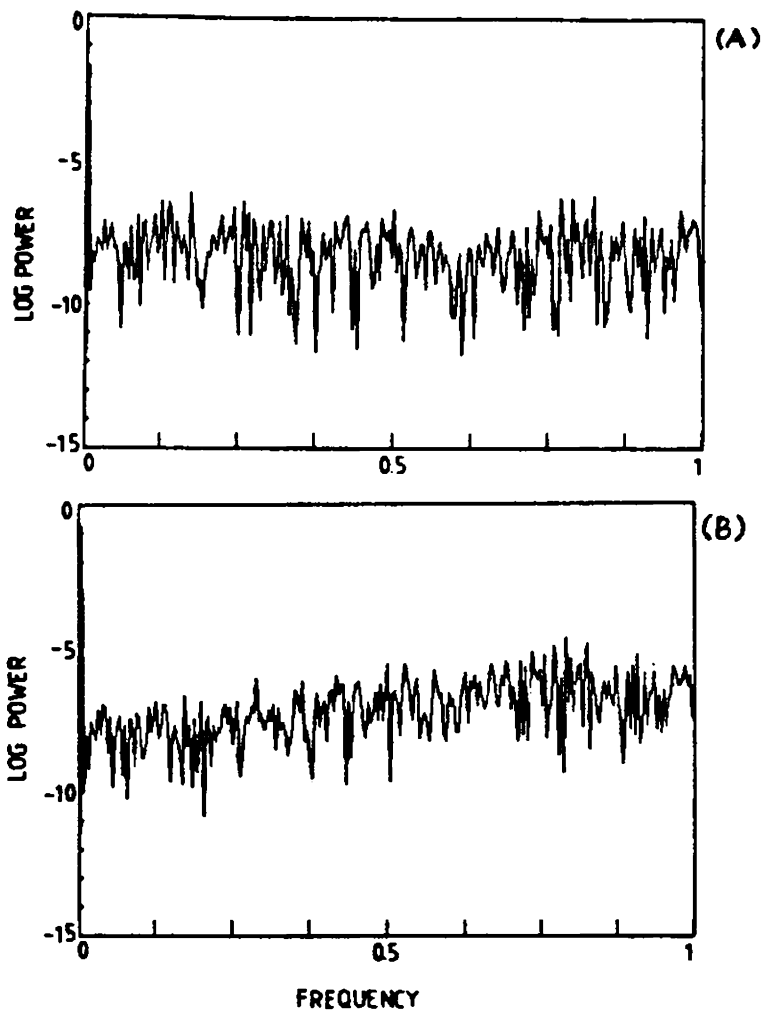


Fig. 11 The power spectrum for the (A) modulated and (B) ordinary logistic map for the parameter value  $\mu = 0.98$ .

parameter has been studied by Giesel et.al [62], using an approximate renormalisation procedure. As expected, they take negative values for  $\mu < \mu_{\infty}$ , whereas in the chaotic region their values become predominantly positive. Huberman and Rudnick [63] have studied the LE for chaotic bands and found a power law behaviour as a function of the control parameter. Here we calculate the LEs of our model to see how the chaotic behaviour of the logistic map is affected by the modulation. Since the map is two dimensional, we can define two LEs,  $\sigma_1$ , and  $\sigma_2$ , one for the  $X$ -degree of freedom and the other for the  $\lambda$ - degree of freedom. Also, the LE for  $\lambda$ , say  $\sigma_2$ , will be same as that of the logistic map. In order to calculate  $\sigma_1$  and  $\sigma_2$ , let us first consider the Jacobian matrix of the map:

$$J(X, \lambda) = \begin{bmatrix} 4\lambda(1-2X) & 4X(1-X) \\ 0 & 4\mu(1-2\lambda) \end{bmatrix}$$

The rate of change of an infinitesimal area by the application of the map is given by the determinant of  $J(X, \lambda)$  which, in our case, is different at different points along an orbit. Note that the amount by which the area is stretched or compressed along the two coordinate directions are given by the eigen values  $A_1$  and  $A_2$  of  $J(X, \lambda)$  since  $|J| = A_1 A_2$ .

Taking the product of the Jacobian matrices  $J(X_i, \lambda_i)$  at  $N$  iterates of the map and letting  $N \rightarrow \infty$ , the average rate of stretching or compression along the  $X$  and  $\lambda$  directions are given by

$$L_1 = \lim_{N \rightarrow \infty} \left| \prod_{i=1}^N A_1^{(i)} \right|^{1/N} \quad (81)$$

$$\text{and } L_2 = \lim_{N \rightarrow \infty} \left| \prod_{i=1}^N A_2^{(i)} \right|^{1/N} \quad (82)$$

where  $A_1^{(i)}$  and  $A_2^{(i)}$  are simply the diagonal elements of  $J(X_i, \lambda_i)$  given by

$$A_1^{(i)} = 4 \lambda_i (1 - 2 X_i) \quad (83)$$

$$\text{and } A_2^{(i)} = 4\mu (1 - 2 \lambda_i) \quad (84)$$

As we know  $L_1$  and  $L_2$  are called Lyapunov numbers whose logarithm give the two LEs  $\sigma_1$  and  $\sigma_2$ . It is easy to see that the LEs of our map are independent of the initial conditions since almost all initial conditions are attracted towards a unique attractor in the unit square. We now compute  $\sigma_1$  and  $\sigma_2$  numerically for several values of  $\mu$  in the range  $\mu = 0.84$  to  $\mu = 1$ . The method we use has been frequently employed in the literature [20,6] for the numerical estimation of the LE.

We fix a particular parameter value for the map. Starting from an initial value  $(X_1, \lambda_1)$ , we

iterate the map  $N$  times and calculate the Jacobian at all these  $N$  iterates. By taking the product of these  $N$  matrices, we get a  $2 \times 2$  matrix, say,  $M$ . If  $\Lambda_1$  and  $\Lambda_2$  are the eigen values of  $M$ , then we have  $\Lambda_1 = \prod_{i=1}^N A_1(i)$  and  $\Lambda_2 = \prod_{i=1}^N A_2(i)$ .

Calculating  $\Lambda_1$  and  $\Lambda_2$ , we can evaluate the quantities  $(1/N) \ln |\Lambda_1|$  and  $(1/N) \ln |\Lambda_2|$ . Repeating this for several  $N$  values, we plot these quantities against  $N$  separately. The same is repeated for other  $\mu$  values and the results are shown in figures 12 and 13. From the behaviour of the graph, we see that  $(1/N) \ln |\Lambda_1|$  and  $(1/N) \ln |\Lambda_2|$  settle down to almost constant values as  $N \rightarrow \infty$ , which serve as an approximate estimate of the LE and can be directly read from the graphs.

A comparison of figures 12 and 13 reveals some interesting features. As expected,  $\sigma_2$  is negative in the regular region and becomes positive as  $\mu$  crosses over to the chaotic phase. At  $\mu=0.96$ ,  $\sigma_2$  is negative indicating the existence of a periodic window, where the behaviour is once again regular. As we increase  $\mu$ ,  $\sigma_2$  increases steadily

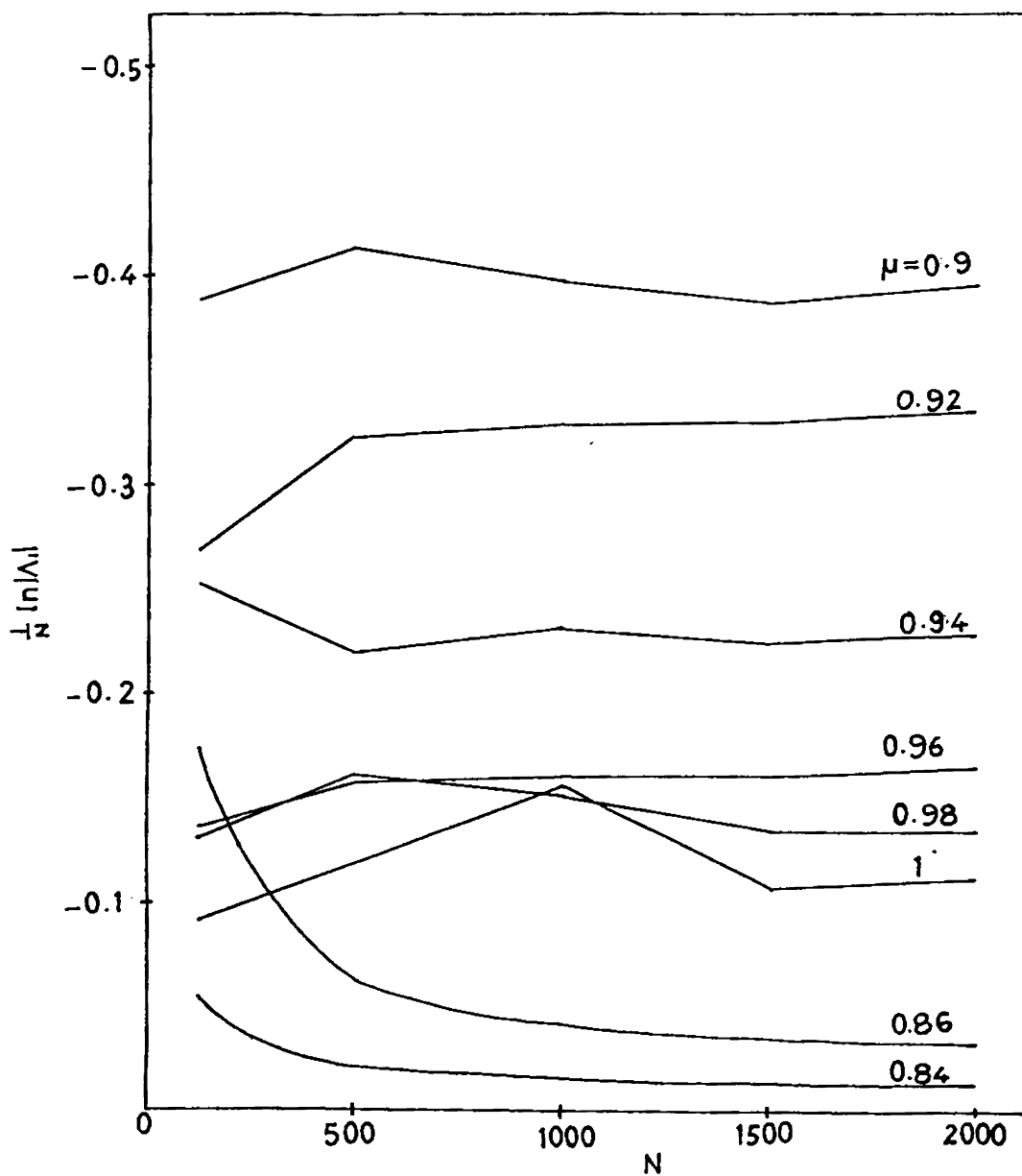


Fig. 12 An approximate numerical estimation of the Lyapunov exponent of the MLM for the X-degree of freedom. Note that it is negative for all values of  $\mu$ .

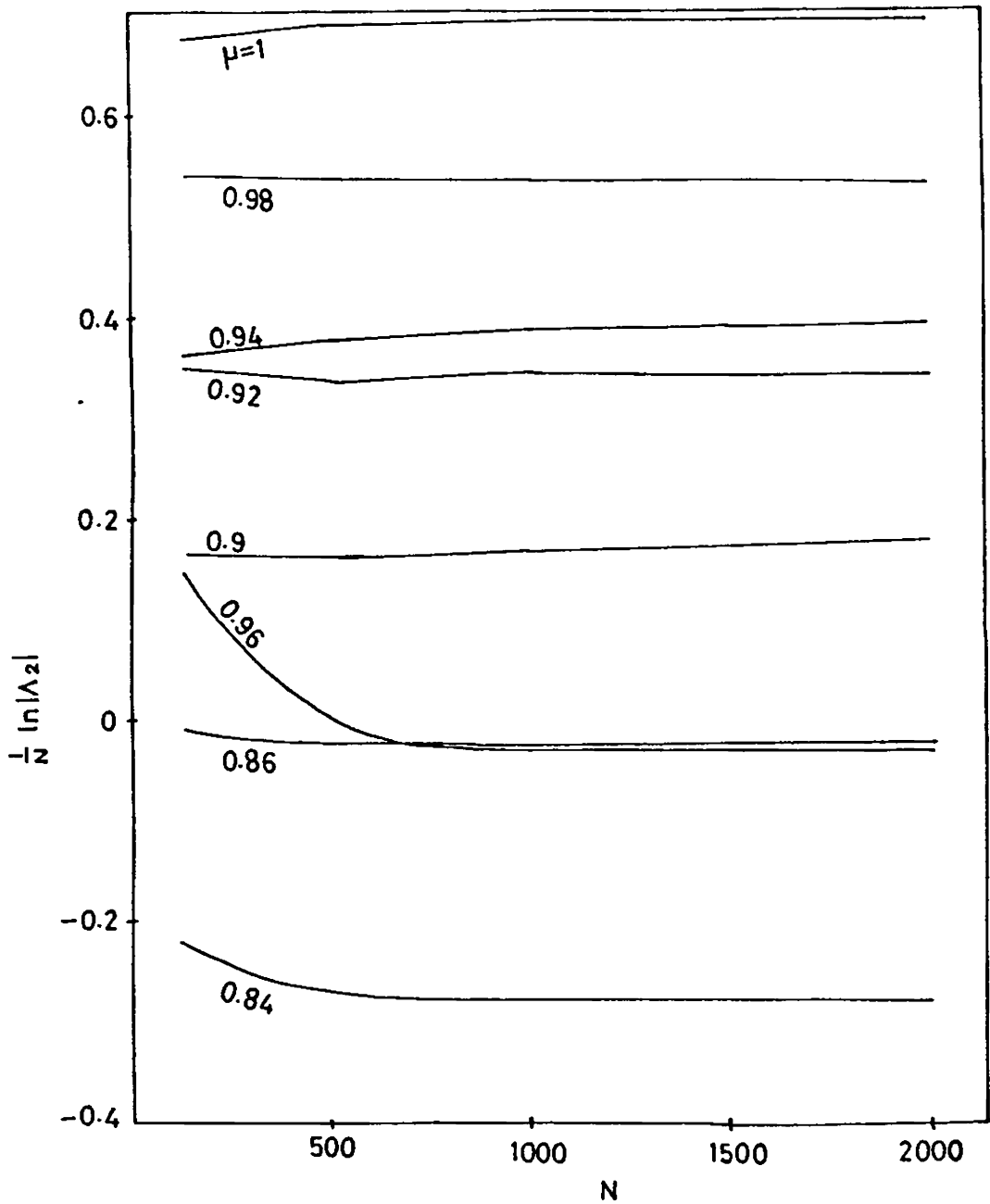


Fig. 13 Lyapunov exponent for the  $\lambda$ -degree of freedom which is same as that of the logistic map. As  $\mu$  increases to  $\mu_{\infty}$ , and above, the LE cross over from a negative to positive value reaching  $\ln 2$  for  $\mu = 1$ .



and reaches a value  $\sim \ln 2$  corresponding to  $\mu=1$ . (There are several periodic windows in between with negative  $\sigma_2$  values which cannot be seen in our graph). The behaviour of  $\sigma_1$  is quite different. It is always negative irrespective of whether  $\mu$  is in the regular region or chaotic region. It has a small negative value in the regular region and reaches its maximum when the system just crosses over to the chaotic state. With further increase in  $\mu$ , its value is reduced. The reason why  $\sigma_1$  is always negative may be that the X-direction is always folded under the mapping, as we see below.

Now, LE is a measure of the exponential separation of nearby points in phase space and hence is proportional to the rate of loss of information regarding the state of the system [5]. Also, the degree of chaos in a system can be measured in terms of this rate of loss of information. The rate of loss of information contained in an infinitesimal unit cell of phase space of the logistic map as well as the MLM is same and is proportional to  $\sigma_2$ . But note that in the case of the logistic map, this interval is 1-dimensional of length, say,  $\epsilon$  whereas in MLM this much amount of information is lost from a square

of side  $\xi$ . In this sense, the 'modulated' logistic map is less chaotic compared to the logistic map. It is interesting to note that this result is in agreement with the observation by Tomita [64], who has studied the same model with  $\mu \sim 1$ , even though in a different context. He used the system as an example of unilateral chaotic modulation to show that the degree of chaos can be reduced by an appropriate modulation or coupling.

#### 4.2 The strange attractors of the map

In this section we show the existence of strange attractors for MLM for many values of the parameter (in fact uncountable in number, as we shall see below). In order to decide whether an attractor is periodic or chaotic, one must look at the spectrum of LEs characterising the attractor. We have seen that, of the two LEs  $\sigma_1$  and  $\sigma_2$  of the map,  $\sigma_1$  is always negative independent of the value of  $\mu$ . This indicates that when  $\sigma_2 > 0$ , the attractor can possibly be 'strange' due to the stretching and folding of the trajectories on the unit square. We now choose one such value, say,  $\mu = 0.895$  and show the corresponding attractor in fig. 14a by plotting 8000 points after the initial 5000 points were discarded. Taking a small region

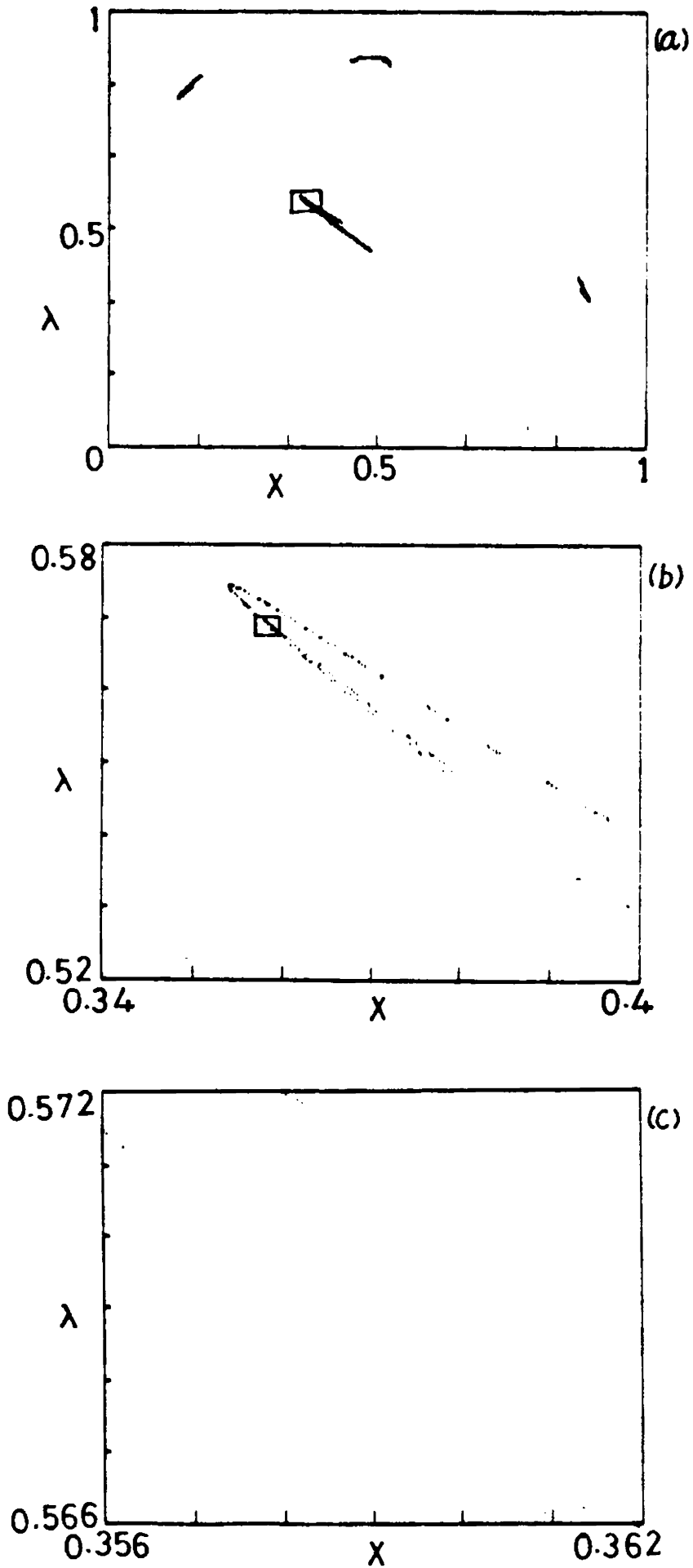
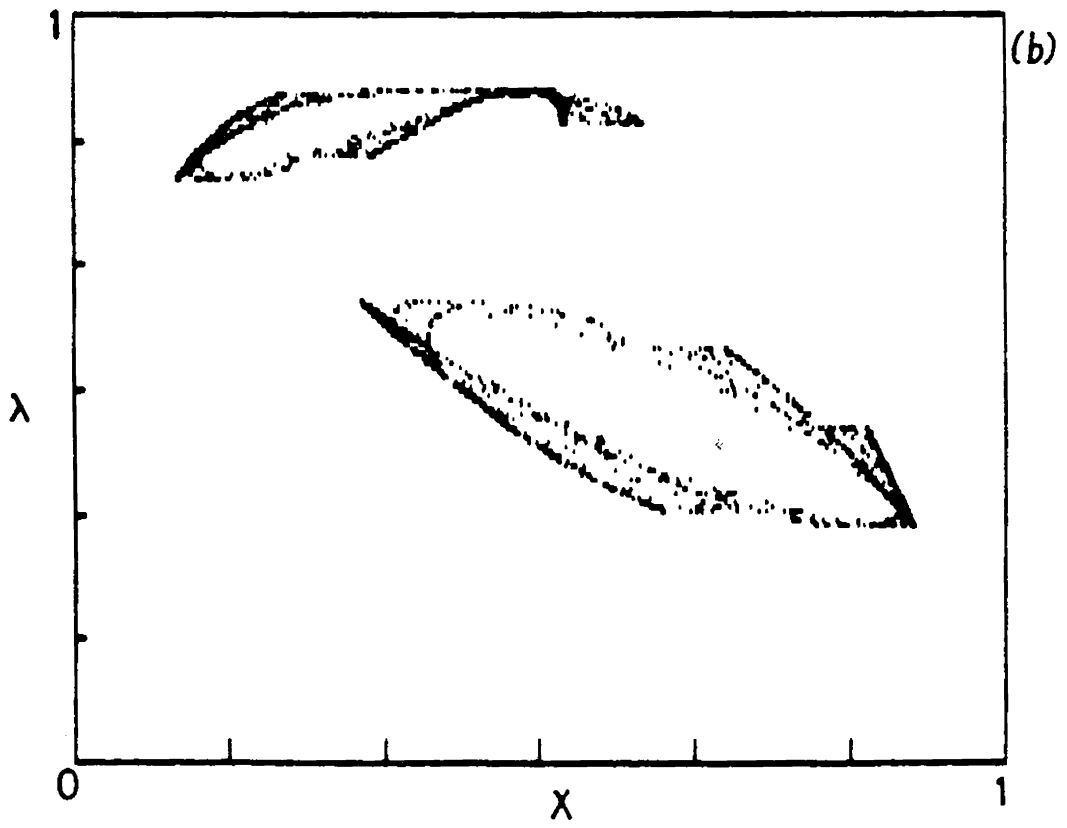
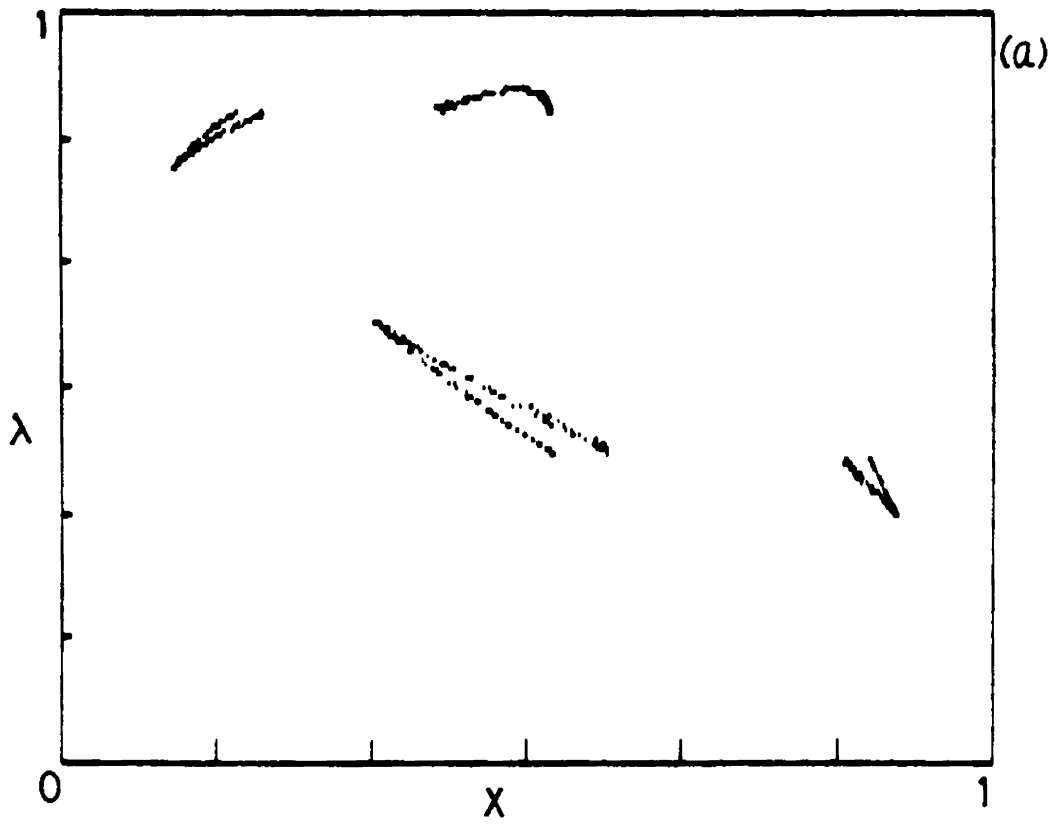
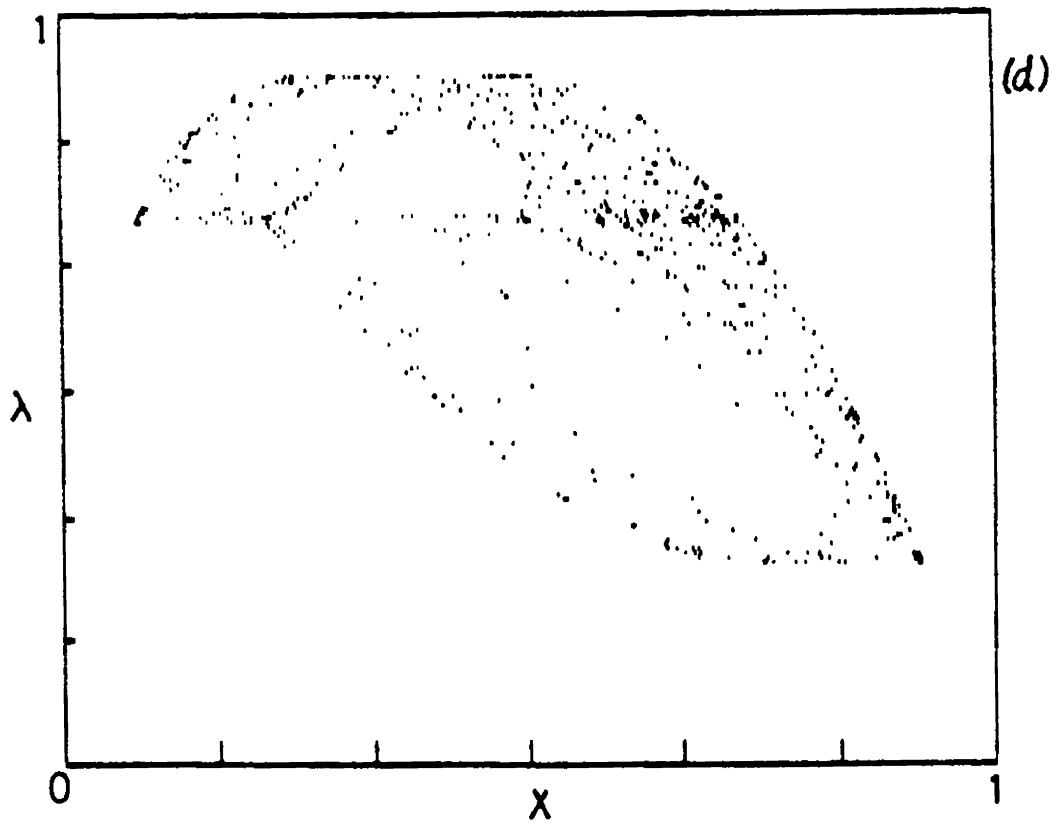
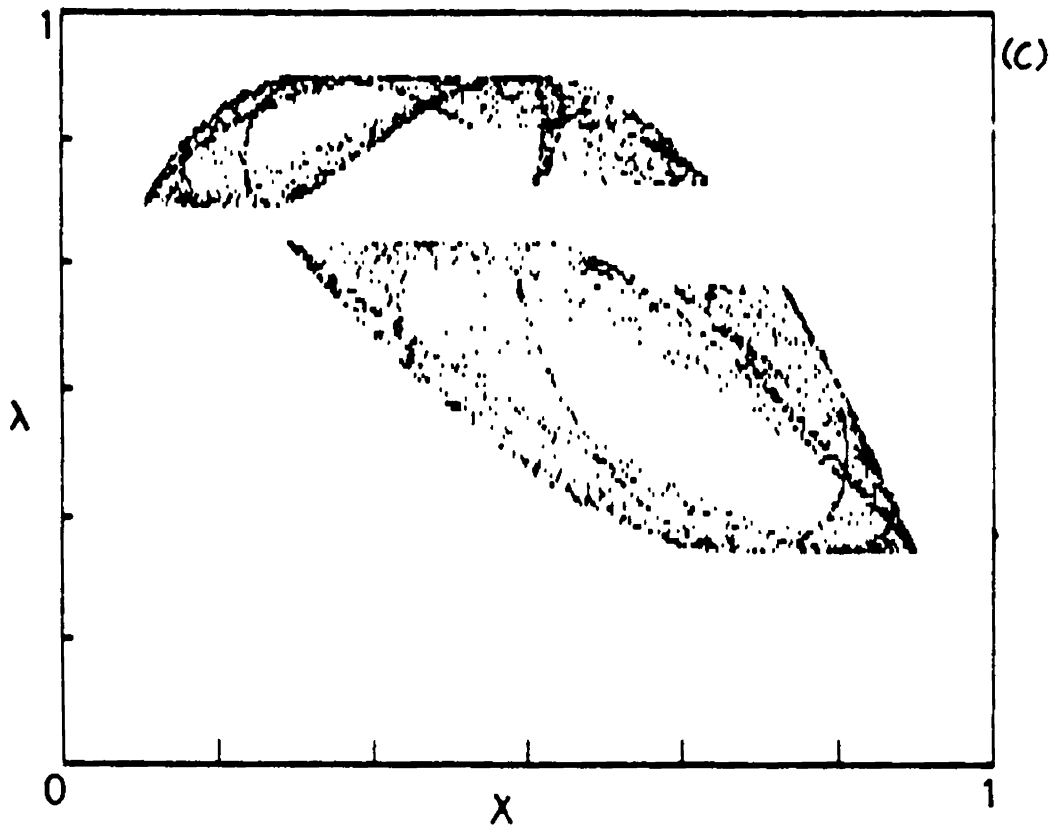


Fig. 14 A plot of the attractor of MLM and its self similar structure for  $\mu = 0.895$ .

of the attractor<sup>1</sup> indicated by a box in the figure and enlarging it we get fig. 14b and repeat this process once again to get fig. 14c. From the figures, it becomes clear that the attractor has a self similar structure, which is in fact very much similar to that of the Henon attractor [26]. We can also give a simple reason to support this numerical evidence. From the Cantor set structure of the  $\lambda$ -values in the interval  $[0,1]$  for  $\sigma_2 > 0$ , it directly follows that any two arbitrarily close points on the attractor will have another point in between (for sufficiently large number of iterations) making the attractor 'self similar'. But it is found that the self similar structure becomes less pronounced within the limits of numerical precision for larger values of the parameter. The reason for this can be attributed to the observed variation in the values of  $\sigma_1$  and  $\sigma_2$  with  $\mu$ , shown in fig. 16 below.

We now present in fig. 15 the numerical plot of the attractor for six different values of  $\mu$ . For  $\mu$  just beyond  $\mu_\infty$ , the attractor consists of several disjoint sets and finally becomes a single piece for sufficiently large value of  $\mu$ . This structure variation necessarily reflects the band merging in the logistic map. Now, the values of  $\mu$  for which





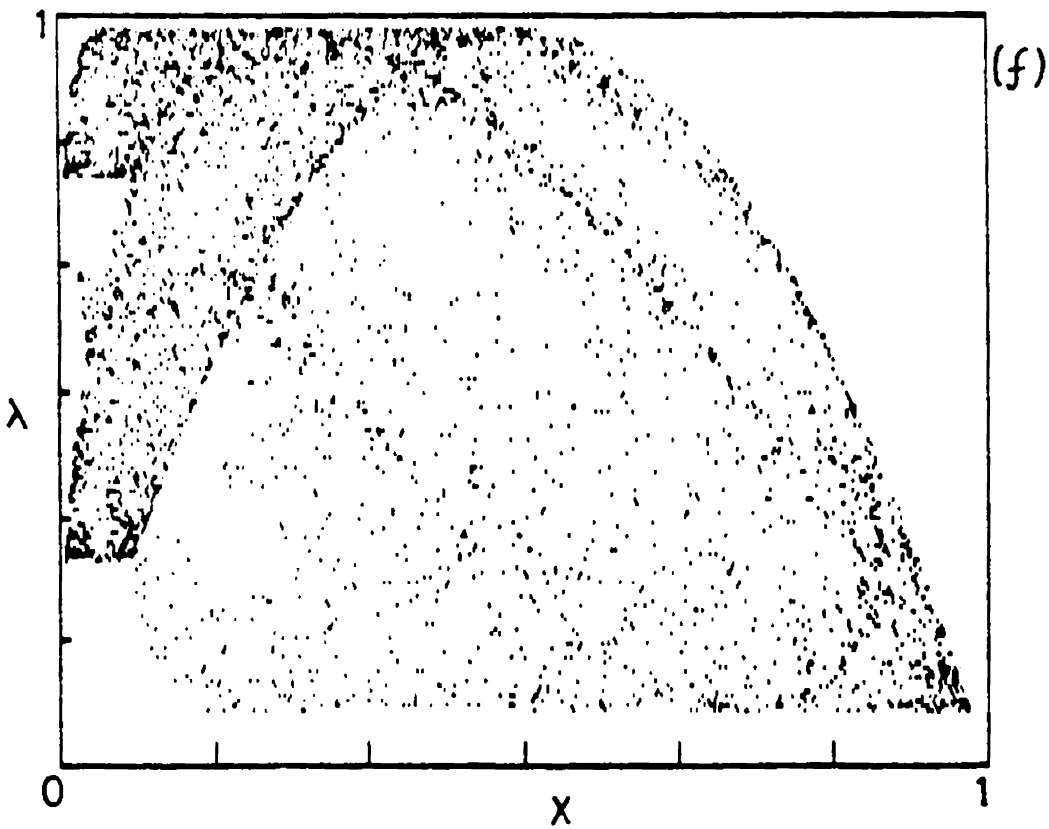
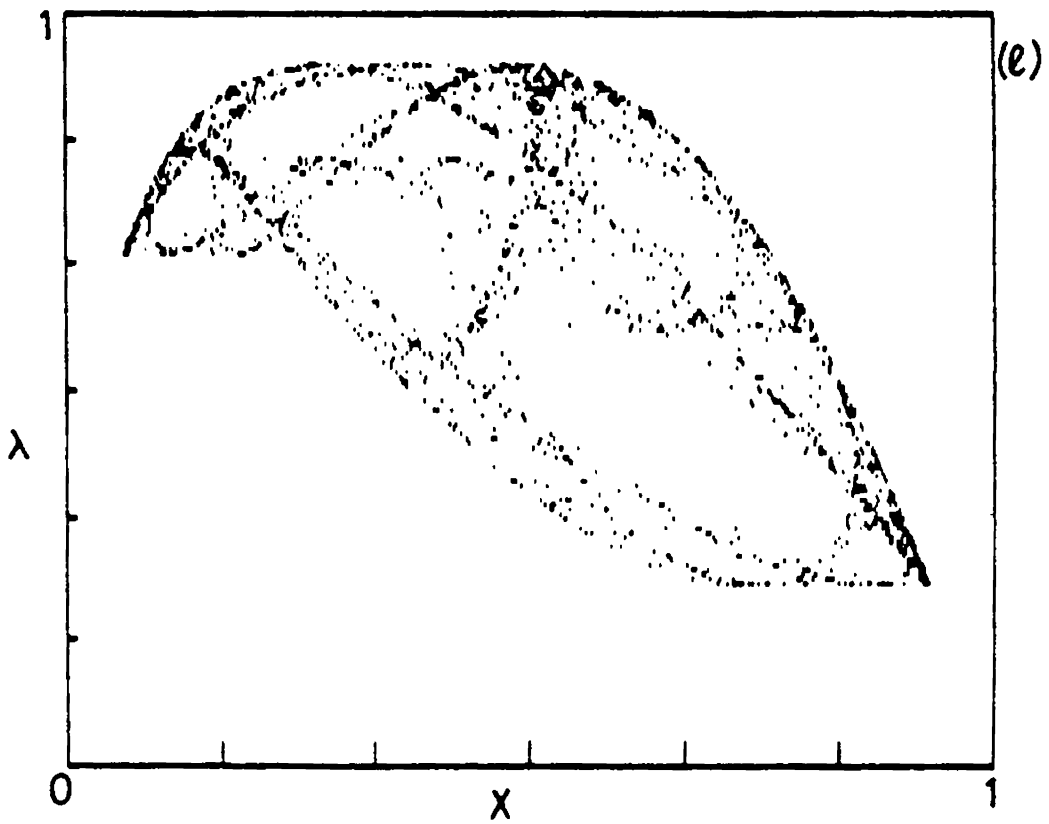


Fig. 15 Strange attractors of MLM for parameter values  
 (a) 0.898; (b) 0.903; (c) 0.915; (d) 0.92;  
 (e) 0.93 and (f) 0.98.

$\sigma_2 > 0$  are uncountable in number and form a set of positive measure on the parameter axis [65,57]. So, in principle, the map can be said to generate uncountable number of strange attractors in the unit square apart from the infinite number of periodic cycles already shown. Here, we want to make one point clear. It is seen from figure 16 below that for sufficiently large values  $\mu$ , the sum of LEs is larger than zero implying that the area elements grow on the average. But we call the resulting fractal set a 'strange attractor' because it satisfies the other properties of an attractor. For example, it is a bounded region to which almost all other initial conditions in the unit square get attracted asymptotically. Moreover, it forms an invariant set whose every part is eventually visited by the iterates. It should be noted that a basic factor responsible for the existence of these 'attractors' with growing area elements is the confinement of the mapping to the unit square. This is discussed in more detail below.

#### 4.3 Fractal and information dimensions

One important question regarding a strange attractor is its dimension. Eventhough there are a variety of different definitions of dimension, the



most relevant ones are i) the fractal dimension, depending only on the metric properties and ii) the information dimension which depends on metric as well as probabilistic properties. The fractal dimension of a set is given by

$$D_0 = \lim_{\epsilon \rightarrow 0} \frac{\log N(\epsilon)}{\log(1/\epsilon)} \quad (85)$$

where, if the set in question is a bounded subset of a  $m$ -dimensional Euclidean space  $R^m$ , then  $N(\epsilon)$  is the minimum number of  $m$ -dimensional cubes of side  $\epsilon$  needed to cover the set. The fractal dimension is only a measure of the 'strangeness' of an attractor and says nothing about the dynamics on it. From figure 15 it can be easily seen that some regions of the attractor are more frequently visited by the trajectories than others. So, in order to understand the dynamics on a chaotic attractor, one must also take into account the distribution or density of points on the attractor. This is more precisely discussed in terms of the information dimension and is given by

$$D_1 = \lim_{\epsilon \rightarrow 0} \frac{I(\epsilon)}{\log(1/\epsilon)} \quad (86)$$

$$\text{where } I(\epsilon) = \sum_{i=1}^{N(\epsilon)} P_i \log(1/P_i) \quad (87)$$

and  $P_i$  is the probability contained within the  $i^{\text{th}}$  cube. It can be easily shown that  $D_0 \geq D_1$ , where

the equality sign holds if the attractor is uniform.

In order to compute these quantities, we made use of the familiar box counting algorithm [18]. The unit square was partitioned into boxes of side  $\epsilon$ . The number of boxes  $N$  which contained at least one point of the attractor as well as the number of points  $\eta_i$  contained in each box were then counted. The probability  $P_i$  is given by  $\eta_i/\eta$  where  $\eta$  is the total number of points on the attractor. Calculating  $N(\epsilon)$  and  $I(\epsilon)$  for various values of  $\epsilon$  and plotting  $\ln N(\epsilon)$  and  $I(\epsilon)$  separately against  $\ln(1/\epsilon)$ ,  $D_0$  and  $D_1$  were obtained as the asymptotic slopes respectively. Our results are presented in table II and in all cases  $D_0 > D_1$  as is required.

We know that the dimension of a set depends on its structure or distribution of points in it. For example, the dimension of a Cantor set depends very much on the way it is constructed [15]. Strange attractors can exhibit a wide variety of shapes and the complexity of these shapes will be related in some way to the relative amounts of stretching and compression which in turn depends on the LEs. To see this possible dependence of the dimension on the LEs, we plot the numerically calculated values of  $\sigma_1$  and  $\sigma_2$  as a function of the parameter  $\mu$  in fig. 16.

Table II Fractal and information dimensions of the strange attractors of MLM for various parameter values

$\mu$	$D_0$	$D_1$
0.895	0.94545	0.92920
0.898	1.04571	1.02326
0.9	1.09677	1.08572
0.903	1.20536	1.1500
0.915	1.4400	1.4080
0.92	1.06666	1.05620
0.93	1.23188	1.19492
0.94	1.30435	1.2500
0.98	1.33928	1.32121
0.995	1.58819	1.5160

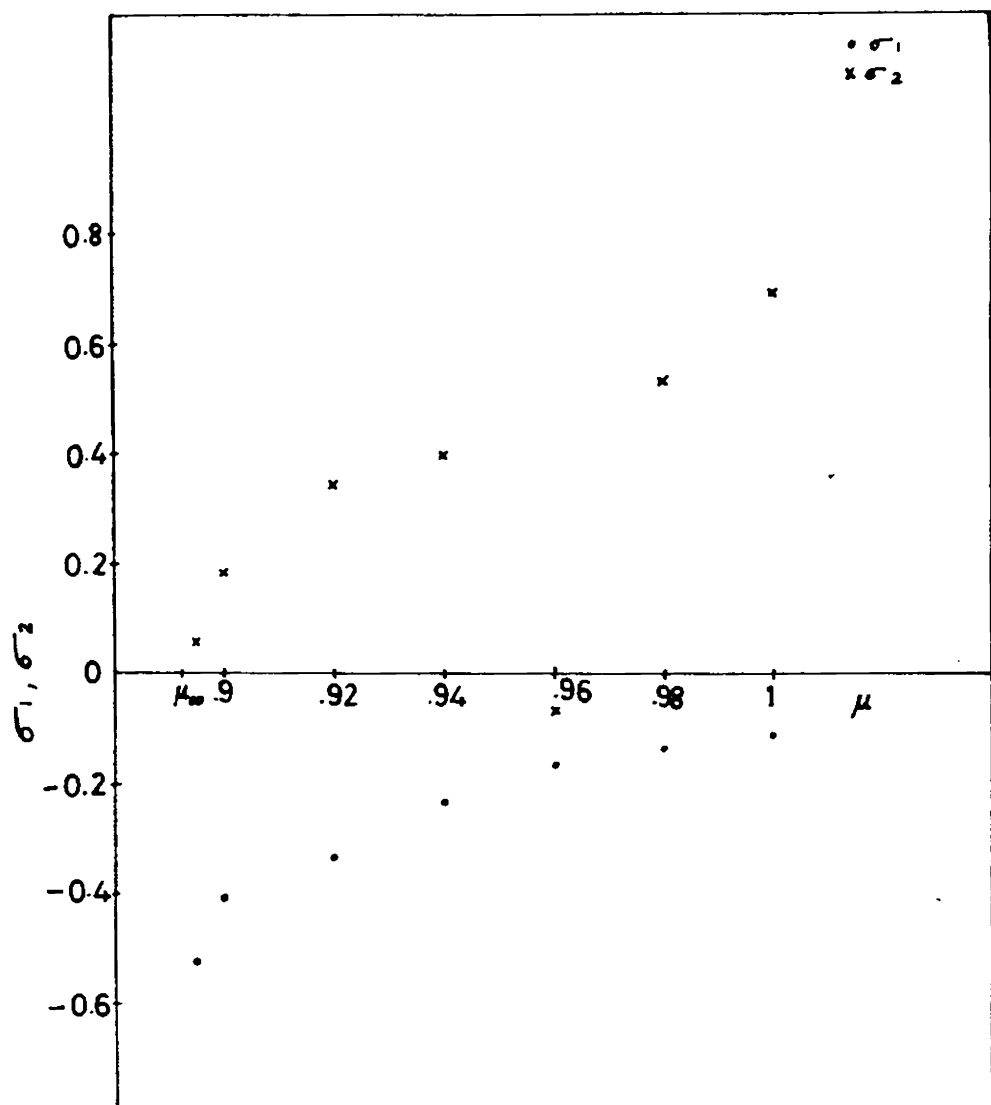


Fig. 16 Lyapunov exponents  $\sigma_1$  and  $\sigma_2$  of MLM for various values of  $\mu$ . This is only to show the variation of the positive values of  $\sigma_2$  and the corresponding values of  $\sigma_1$  with  $\mu$ .

We have shown only a few positive values of  $\sigma_2$  and the corresponding values of  $\sigma_1$ . In between, there are infinite number of  $\mu$  values with  $\sigma_2 < 0$  of which only one corresponding to the period 3 window is given. From the variation of  $\sigma_1$  and  $\sigma_2$ , it becomes clear why the strange attractor becomes more and more stretched out as  $\mu$  increases.

Now, it is well known that a direct estimation of the dimension  $D_1$  of the strange attractor can be made in terms of the LEs making use of the Kaplan-Yorke conjecture [66,18]. However, it is found that this is not possible for the MLM. We now show that, this is due to a typical property of noninvertible maps bounded on an interval. As a first step, note from figure 16 that for larger values of  $\mu$ ,  $\sigma_1 + \sigma_2 > 0$  which implies that the stretching is globally predominant. For an  $N$ -dimensional flow or the related  $(N-1)$ -dimensional invertible map to be chaotic, the largest LE should be  $> 0$  while  $\sum_i \sigma_i < 0$  [6,67], implying that the phase space volume must contract globally. The main point is that for such systems, there is a well defined condition in terms of the LEs which determines

the existence of a strange attractor. Now, for noninvertible maps on an interval, this link between the volume contraction and the exponential divergence of nearby trajectories is broken [6]. For such systems, a bounded chaotic motion can occur even if  $\sum_i \sigma_i > 0$  as is evident from our map. The reason for this depends crucially on the fundamental property of transformation, namely, the noninvertibility. While the sensitive dependence on initial conditions stretches any small initial displacement by an average stretching factor resulting in an exponential increase in the displacement, the noninvertibility helps the mapping to remain bounded in the interval. To see how this happens in our map, note that points lying on a line parallel to the X-axis are mapped on to another line parallel to it. Moreover, for every point on the first half of the initial line, there is a symmetric point on the second half, both being mapped on to a single point, implying compression along the X-direction. Now, it can be easily seen that half of the interval with  $\lambda$  in the range  $0 < \lambda < 1/2$  is stretched along the opposite direction by an amount which increases with the value of  $\mu$ . So, when  $\mu$  is sufficiently large, the whole plane should be folded back into the unit square about

a line parallel to the X-axis, in order to remain bounded in it. The whole process of confinement is analogous to that in the quadratic map which has been discussed in detail by Berge et.al [4]. In fact, they show that noninvertibility is essential for a mapping of  $R$  into  $R$  to be capable of producing chaos. It is then evident that this fundamental property does play a role along with the sensitive dependence on initial conditions in the formation of strange attractors in MLM. So, it is not surprising that a direct relationship connecting the fractal dimension and the LEs, such as the one conjectured by Kaplan and Yorke, does not exist for our map. This is also in agreement with the fact that the conjecture has been shown to hold only for those maps for which the phase space volume contracts after each iteration ( $\sum_i \sigma_i < 0$ ) and the contraction is, in fact, uniform everywhere [68, 6].

Finally, for a more complete physical characterisation of strange attractors we require the knowledge of the generalised fractal dimensions  $D_q$  [17]. They can also be used to obtain a global scaling measure of the strange attractor. The fact

that  $D_0$  and  $D_1$  are greater than one indicates that MLM may be useful in studying certain higher dimensional chaotic phenomena.



## V. CONCLUDING REMARKS

It is well known that first order nonlinear difference equations such as the logistic map arises naturally in several areas ranging from mathematical economics to population biology [2,27]. There are of course numerous instances where the dynamics of a complex system is intrinsically multidimensional, in the sense that more than one dynamical variable is needed for a complete specification of the state of the system. This is why studies on various kinds of coupled and modulated maps have been gaining more and more interest recently [69,70,71]. We have analysed two coupled first order difference equations of the logistic type which are confined to the unit square. The onset and characterisation of chaos in this model have been thoroughly investigated.

The map follows the period doubling route to chaos as the control parameter is increased and also shows the universal scaling properties of quadratic maps at the onset of chaos. The bifurcation structure itself has some novel features compared to that of

the logistic map. Another interesting property of our map is the existence of infinite number of periodic windows which are arranged along the parameter axis exactly in accordance with the Sarkovskii ordering. The importance of this result is that it is widely believed to be only a 1D result because no higher dimensional map is currently known to obey Sarkovskii ordering.

We have also made extensive analysis of the chaotic region of the map and have shown that the model can generate strange attractors in the unit square for an uncountable number of parameter values in the range  $\mu_{\infty} < \mu < 1$ . Numerical plot of strange attractors for several values of  $\mu$  are given and their fractal and information dimensions are calculated. It is found that their values are greater than one in almost all cases. All these results combine to suggest that our model can be considered as an analogue of the logistic map in two dimensions and may be useful in describing certain higher dimensional chaotic phenomena.

The importance of modulation maps have been stressed by many authors recently. Ruelle[47] has proposed an exactly similar kind of model for the

study of some of the currently interesting chaotic systems. At present, most of our knowledge regarding the behaviour of chaotic systems comes from the study of 1D noninvertible maps and 2D invertible maps [72,57]. Comparatively, studies on 2D noninvertible maps are very few and their properties are less well understood today. At the same time, chaotic behaviour is being discovered in a variety of new systems and their number is increasing day by day. Most of these systems are complex enough not to allow a description in terms of simple 1D maps. A recent example is the discovery of chaos in electrical discharges by Braun et.al [73], where the authors have stressed the need of a 2D map as a useful model for the system.

There are also situations where a 2D map can naturally arise as a model for the system dynamics. As we have already seen in Chapter II, the Poincaré section of a highly dissipative 3D flow can often be reduced to a noninvertible map of the line  $\mathbb{R}$  into itself. It is called a first return map of the form

$$X_{n+1} = f(X_n).$$

But in certain cases, the function  $f(X)$  appears to cross itself or tangled indicating that the dynamics

is embedded in a higher dimensional space. A second order mapping function of the form

$$X_{n+2} = f(X_{n+1}, X_n)$$

is then made use of to unravel the essential features of the system. A familiar example is the study of circuits with p-n junctions [74]. The above second order difference equation is completely equivalent to a 2D mapping. Our model also can be written as a second order difference equation in  $X$  whose evolution can be obtained by specifying  $X_0$  and  $X_1$ . Recently, Moon [75] has discussed several examples of chaotic systems where a second order mapping function is made use of to determine the underlying dynamics of the system.

Perhaps the most important result that we have shown for our model is that it comes under the universality class of Feigenbaum. This result implies that an important factor for the realisation of universal scaling properties is the confinement of the dynamics to an interval, whether it is in  $R$  or in  $R^2$ . As we know, the infinite sequences of period doubling bifurcations with Feigenbaum scaling have been observed in several higher dimensional chaotic systems [14]. A standard example is the Lorenz model,

eventhough a number of new systems have recently been identified [75]. In the case of the Lorenz system, it is assumed that the solutions of the system, which are identified as the trajectories in phase space, are uniformly bounded as  $t \rightarrow \infty$ . That is, there is a bounded region such that every trajectory ultimately remains with it, analogous to the dynamics in our model. This shows that our result may well be a key in understanding why the universal scaling properties exist in such bounded or 'closed flow' systems.

Before concluding this thesis, we also indicate some of the possibilities for future investigations along the same line. Our studies were basically centered around a single model, a modulated logistic map. It will be more interesting to analyse a class of such modulation maps using, for example, other simple nonlinear functions for the evolution of  $\lambda$ . We can possibly study the dependence of scaling properties on the specific form of the modulation map. It will also be interesting to see whether there exists a one parameter family of 2D maps, as in the 1D case, having the same universal properties. This will enable us to obtain some generic features of the chaotic behaviour in higher dimensional systems.

## References

- [1] M. Henon in Chaotic Behaviour of Deterministic Systems (Eds.) G. Iooss, R.H.G. Helleman and R. Stora (North-Holland, Amsterdam, 1983) p. 53.
- [2] R.M. May, Nature 261 (1976) 459.
- [3] E.N. Lorenz, J. Atmos. Sci. 20(1963) 130.
- [4] P. Berge, Y. Pomeau and C. Vidal, Order within Chaos (John Wiley, New York, 1986).
- [5] H.G. Shuster, Deterministic Chaos - An Introduction (Physik Verlag, Weinheim, 1984).
- [6] A.J. Lichtenberg and M.A. Lieberman, Regular and Stochastic Motion (Springer, Berlin, 1983).
- [7] J.P. Eckmann and D. Ruelle, Rev. Mod. Phys. 57 (1985) 617.
- [8] W.H. Press, B.P. Flannery, S.A. Teukolsky and W.T. Vetterling, Numerical Recipes (Cambridge University Press, Cambridge, 1986).
- [9] D. Ruelle and F. Takes, Commun. Math. Phys. 20 (1971) 167.
- [10] S. Newhouse, D. Ruelle and F. Takens, Commun. Math. Phys. 64 (1978) 35.
- [11] Y. Pomeau and P. Manneville, Commun. Math. Phys. 74 (1980) 189.
- [12] M.J. Feigenbaum, J. Stat. Phys. 19(1978) 25.
- [13] M.J. Feigenbaum, J. Stat. Phys. 21(1979) 669.

- [14] B.L. Hao, Chaos (World Scientific, Singapore, 1984).
- [15] B.B. Mandelbrot, Fractals: Form, Chance and Dimension (Freeman, San Francisco, 1977).
- [16] B.B. Mandelbrot, The Fractal Geometry of Nature (Freeman, San Francisco, 1982).
- [17] H.G.E. Hentschel and I. Procaccia, Physica D 8 (1983) 435.
- [18] J.D. Farmer, E. Ott and J.A. Yorke, Physica D 7 (1983) 153.
- [19] V.I. Oseledec, Trans, Moscow Math. Soc. 19 (1968) 197.
- [20] G. Benettin, L. Galgani and J.M. Strelcyn, Phys. Rev. A14 (1976) 2338.
- [21] G. Benettin, L. Galgani, A. Giorgilli and J.M. Strelcyn, Meccanica 3 (1980) 21.
- [22] I. Shimada and T. Nagashima, Prog. Theor. Phys. 61 (1979) 1605.
- [23] See the collected papers in Proc. R. Soc. Lond. A413 (1987).
- [24] J.P. Gollub and S.V. Benson, J. Fluid. Mech. 100 (1980) 449.
- [25] J.C. Roux, R.H. Simoyi and H.L. Swinney, Physica D8 (1983) 257.
- [26] M. Henon, Commun. Math. Phys. 50 (1976) 69.

- [27] R.M. May in Chaotic Behaviour of Deterministic Systems (Eds.) G.Iooss, R.H.G. Helleman and R. Stora (North-Holland, Amsterdam, 1983) p. 513.
- [28] M.J. Feigenbaum, Los Alamos Sci. 1 (1980) 4.
- [29] C. Grebogi, E. Ott and J.A. Yorke, Phys. Rev. Lett. 48 (1982) 1507.
- [30] S.D. Feit, Commun. Math. Phys. 61 (1978) 249.
- [31] C. Simo, J. Stat. Phys. 21 (1979) 465.
- [32] J.H. Curry, Commun. Math. Phys. 68 (1979) 129.
- [33] D.L. Hitzl, Physica D 2 (1981) 370.
- [34] D.L. Hitzl, Physica D 14 (1985) 305.
- [35] H. Froehling, J.P. Crutchfield, J.D. Farmer, N.H. Packard and R. Shaw, Physica D 3 (1981) 605.
- [36] T.C. Bountis, Physica D 3 (1981) 577.
- [37] V. Franceschini and C. Tebaldi, J. Stat. Phys. 21 (1979) 707.
- [38] O.E. Roßler, Ann. N.Y. Acad. Sci. 316(1979)376.
- [39] B.A. Huberman and J.P. Crutchfield, Phys. Rev. Lett. 43(1979) 1743.
- [40] P. Coullet, C. Tressor and A. Arnéodo, Phys. Lett. A 72 (1979) 268.
- [41] H. Haken, Phys. Lett. A 53 (1975) 77.
- [42] C. Sparrow, The Lorenz Equations: Bifurcations, Chaos and Strange Attractors (Springer, Berlin, 1982).
- [43] J. Guckenheimer and P. Holmes, Nonlinear Oscillations, Dynamical Systems and Bifurcations of Vector Fields (Springer, Berlin, 1983).



- [44] J. Guckenheimer, G.F. Oster and A. Ipaktchi, *J. Math. Biol.* 4 (1976) 101.
- [45] J.R. Tredicce, N.B. Abraham, G.P. Puccioni and F.T. AVECCHI, *Opt. Commun.* 55 (1985) 131.
- [46] E. Brun, B. Derighetti, R. Holzner and D. Meier in *Optical Bistability* (Eds.) C.M. Bowden, H.M. Gibbs and S.L. McCall (Plenum, New York, 1984) p. 127.
- [47] D. Ruelle, *Proc. R. Soc. Lond. A* 413(1987) 5.
- [48] P. Mandel and T. Erneux, *Phys. Rev. Lett.* 53 (1984) 1818.
- [49] R. Kapral and P. Mandel, *Phys. Rev. A* 32(1985) 1076.
- [50] B. Derrida, A. Gervois and Y. Pomeau, *J. Phys.* A12 (1979) 269.
- [51] J.M. Greene, *J. Math. Phys.* 9 (1968) 760.
- [52] B. Derrida and Y. Pomeau, *Phys. Lett. A* 80 (1980) 217.
- [53] R.H.G. Helleman in *Fundamental Problems in Statistical Mechanics, Vol. 5*, E.G.D. Cohen (Ed.) (North Holland, Amsterdam, 1980).
- [54] R.H.G. Helleman in *Long Time Prediction in Dynamics*, C.W. Horton Jr., L.E. Reichl and A.G. Szebehely (Eds.) (John Wiley, New York, 1983).
- [55] A.N. Sarkovskii, *Ukr. Math. J.* 16 (1964) 61.

- [56] P. Stefan, *Commun. Math. Phys.* 54 (1977) 237.
- [57] R.L. Devaney, *An Introduction to Chaotic Dynamical Systems* (Benjamin, Menlo Park, 1986).
- [58] T.Y. Li and J.A. Yorke, *Am. Math. Monthly* 82 (1975) 985.
- [59] N. Metropolis, M.L. Stein and P.R. Stein, *J. Comb. Theory* 15 (1973) 25.
- [60] B. Derrida, A. Gervois and Y. Pomeau, *Ann. Inst. H. Poincaré* A29 (1978) 305.
- [61] C. Grebogi, E. Ott and J.A. Yorke, *Physica D* 7 (1983) 181.
- [62] T. Giesel, J. Nierwetberg and J. Keller, *Phys. Lett.* A86 (1981) 75.
- [63] B.A. Huberman and J. Rudnick, *Phys. Rev. Lett.* 45 (1980) 154.
- [64] K. Tomita in *Chaos and Statistical Methods* (Ed.) Y. Kuramoto (Springer, Berlin, 1984).
- [65] J.D. Farmer, *Phys. Rev. Lett.* 55 (1985) 351.
- [66] J. Kaplan and J.A. Yorke in *Lecture Notes in Math.* 730 (Eds.) H.O. Peitgen and H.O. Walther (Springer, Berlin, 1978).
- [67] E.N. Lorenz, *Physica D* 17 (1985) 279.
- [68] D.A. Russel, J.D. Hanson and E. Ott, *Phys. Rev. Lett.* 45 (1980) 1175.
- [69] J.M. Yuan, M. Tung, D.H. Feng and L.M. Narducci, *Phys. Rev.* A28 (1983) 1662.

- [70] R.J. Deissler and K. Kaneko, Phys. Lett. A 119 (1987) 397.
- [71] K. Kaneko, Collapse of Tori and Genesis of Chaos in Dissipative Systems (World Scientific, Singapore, 1986).
- [72] E. Ott, Rev. Mod. Phys. 53 (1981) 655.
- [73] T. Braun, J.A. Lisboa, R.E. Francke and J.A.C. Gallas, Phys. Rev. Lett. 59 (1987) 613.
- [74] R. Van Buskirk and C. Jeffries, Phys. Rev. A31 (1985) 3332.
- [75] F.C. Moon, Chaotic Vibrations (John Wiley, New York, 1987).